

Table 3. List of genes that had significantly different expression levels in NR and NL (fold change <1/3, 3<, and p<0.05).

symbol	NR/NL (fold change)	NR/NL (t-test)	NR/SVR (fold change)	NR/SVR (t-test)
GADD45B	0.20	1.14E-02	1.01	NS
HES1	0.26	1.26E-03	0.97	NS
BCL3	0.26	1.84E-02	1.02	NS
STAT3	0.26	5.81E-04	0.97	NS
SOCS3	0.27	7.96E-03	0.68	2.15E-02
DDX11	0.28	4.33E-05	0.59	9.52E-03
TRIM22	3.06	2.91E-03	1.37	7.97E-03
ASC	3.19	1.35E-03	1.33	4.07E-03
UBE2L6	3.32	1.06E-02	1.41	1.01E-03
STAT1	3.38	6.04E-04	1.33	1.86E-02
ISG20	3.64	2.42E-04	1.42	2.37E-03
TRAIL	3.81	2.08E-02	0.78	NS
OAS2	4.02	2.91E-03	1.89	1.07E-04
IFI2	4.60	1.48E-03	1.56	8.34E-05
BST2(Tetherin)	5.14	8.17E-03	1.49	5.67E-04
IFI35	5.29	1.35E-03	1.63	2.37E-05
HERC5	5.32	1.16E-03	1.68	4.07E-05
MX1	6.21	1.33E-03	2.94	8.46E-07
HLA-C	6.49	6.34E-04	1.21	NS
CCL5(RANTES)	6.73	5.48E-04	1.25	3.77E-02
HLA-B	6.84	4.91E-04	1.22	NS
OAS1	7.80	5.52E-04	2.75	1.92E-04
HLA-A	8.49	5.92E-05	1.41	9.08E-04
B2m	9.09	7.78E-04	1.25	1.89E-02
IFIT1	9.42	1.86E-03	2.11	1.41E-05
OASL	10.38	3.97E-06	1.48	1.24E-02
IFIT3	10.45	4.33E-05	2.11	5.63E-06
CXCL10(IP10)	15.67	8.89E-07	1.28	NS
IFI44	17.00	9.40E-05	2.22	4.83E-06
ISG15	21.12	1.05E-04	2.85	3.99E-05
IFI27	43.74	1.80E-05	2.56	5.62E-05

doi:10.1371/journal.pone.0019799.t003

Genes which participate in IFN production (TLR7, MyD88, IRAK1, and IRF7) did not show any significant difference in their expression level prior to CH combination therapy, and their level at the clinical outcome (Figure 4A and 4B). However, the gene expression pattern of down-stream IFN pathway genes (IFI27, IFI44, ISG15, MX1, and OAS1) was significantly different among SVR, R, and NR (Table 2). IFN is usually up-regulated in HCV infected cells; however in some cases, the mechanism that controls IFN becomes abnormal, and the expression levels of IFN and ISG remain high without any curative effect [23]. The ISG family was generally up-regulated in NR compared to SVR [24–27] and this high expression of ISG related genes was associated with poor response to IFN therapy in previous, as well as in this present study. ISG15 has been linked to innate immune response to viruses and to cellular response to IFN. Although over-expression of ISG15 enhances the antiviral activity of IFN in vitro in acute

infection [28], in chronic infection, extended pre-activation of IFN induced genes leads to dysregulation of the IFN system.

CH therapy is still imperfect at present and therefore suitable prediction methods are necessary to avoid adverse effects. Treatment failure using CH combination therapy is associated with up-regulation of a specific set of IFN-responsive genes thereby making it possible to predict non-response to exogenous therapy [29]. Early gene expression during anti-HCV therapy may elucidate important molecular pathways that might be influencing the probability of achieving a virological response [30]. Our study supports this fact by demonstrating that CH and NL differ fundamentally in their innate response to CH combination therapy.

IFN related gene expression suggests novel aspects of HCV pathogenesis, and form the basis for a subset of genes that can predict treatment response before initiation of combination therapy. After proper external validation, these gene sets may provide the basis for a diagnostic biomarker that can determine early on whether a patient treated with combination therapy is likely to be NR or not. In this respect, what sets our analysis apart is the effect of using DLDA to predict final response with high accuracy in NR and non-NR groups. This prediction showed that the expectation in NR (proportion of actual non-NR versus the predicted number of non-NR) was 93.3% and overall accuracy was 86.1%. In prior report, Dill et al. successfully predicted SVR, but were unable to predict R and NR with high accuracy [31]. In our experiments on the other hand, we predicted NR with high accuracy but were unable to do so for SVR and R. Possible causes for differences between our results and those received by Dill et al. may be (1) the differences in the races of subjects; European patients vs. Japanese patients in our study, (2) the composition of genotype; genotype 1 and 4 vs. genotype 1b in our study, and (3) the difference of the ISG genes extracted.

Genome-wide association studies have described allelic variants near the IL28B gene that are associated with treatment response and with spontaneous clearance of HCV [11–13]. In order to clarify the relationship between IL28B polymorphism and drug response, we compared the expression level of IFN-lambda related gene at the clinical outcome with any genetic variation in IL28B. The expression of hepatic ISG and related genes was strongly associated with treatment response and genetic variation of IL28B [32]. Classification of the patients into SVR and NR revealed that ISG expression was conditionally independent of the IL28B genotype. In CH patients in Europe, the expression pattern of genes induced by IFN more accurately predicts CH combination treatment clinical outcome than polymorphism of IL28B [31]. We observed that curative effect prediction using IFN gene expression pattern resulted in high level of accuracy, however, IFN with IL28B or IFN alone resulted in approximately similar levels of accuracy, therefore, the polymorphism of IL28B did not contribute significantly to our prediction. These findings are accordance with Dill et al. results (Table 7). There was an increased expression in NR compared to SVR irrespective of the IL28B genotype. However, there was no significant difference in their expression at the clinical outcome or in the genetic variation of IL28B (Figure 3A and 3B). Genetic variation of IL28B polymorphism is effective in predicting curative effect; however, the reason for this is not fully understood.

In conclusion, comprehensive analysis of IFN related gene showed that dysregulation of the IFN system might be related to treatment failure and that IFN related gene expression before treatment can enable accurate prediction of CH combination therapy clinical outcome. By focusing the full course of treatment on only those patients who have the highest likelihood of achieving

Table 4. Characteristics of the training and validation set.

	non NR (SVR+R) group		p-value	NR group		p-value
	average (training set)	average (validation set)		average (training set)	average (validation set)	
No.	32	32		12	11	
Age	59.3	57.1	0.38	60.6	61.7	0.74
HCV RNA ($\times 10^6$ IU/ml)	1.77	2.08	0.48	1.51	1.52	0.97
AST (IU/L)	44.6	65.3	0.06	55.3	56.9	0.89
ALT (IU/L)	50	87.3	0.05	67.7	66.8	0.96
WBC ($\times 10^3$ /mm ³)	5220	5440	0.57	4610	4860	0.6
Platelet ($\times 10^4$ /mm ³)	15.8	17.6	0.15	15	15.2	0.95
Total bilirubin (mg/dl)	0.71	0.69	0.78	0.68	0.68	0.92
weight	58.1	59.2	0.67	57	53.8	0.28
ALP (IU/L)	251	249	0.92	298	326	0.64
gGTP (IU/L)	48	57.4	0.54	73.3	73.8	0.98
Hemoglobin (g/dl)	13.9	14.1	0.53	13.7	13.5	0.78
Albumin (g/dl)	4.15	4.21	0.41	4.11	3.98	0.52

doi:10.1371/journal.pone.0019799.t004

SVR, clinicians could potentially reduce the side effects and costs associated with these regimens and provide a more personalized approach to treating CH patients.

Materials and Methods

Patients and sample preparation

Eighty seven CH patients with HCV genotype 1b in the Department of Gastroenterology at the Ogaki Municipal Hospital were enrolled between 2004 and 2006 (Table 1). Patients with autoimmune hepatitis, alcohol-induced liver injury, and patients positive for hepatitis B virus associated antigen/antibody or anti-human immunodeficiency virus antibody were excluded. None of the patients had received IFN therapy or immunomodulatory therapy prior to enrollment. Five normal liver specimens were obtained by surgical resection. Three of these were obtained from Osaka City University Hospital and were taken from gall bladder cancer, cholangiocarcinoma, and hemangioma patients whose liver tissue were normal based on histological, virological and blood examination of their liver function. The remaining two normal liver samples were obtained from the Liver Transplantation Unit of Kyoto University Hospital.

Patients' serum HCV RNA was quantified before IFN treatment using Amplicor-HCV Monitor Assay (Roche Molecular Diagnostics Co., Tokyo, Japan). Histological grading and staging of liver biopsy specimens from the CH patients were performed

according to the Metavir classification system. Pretreatment blood samples were analyzed to determine the level of aspartate aminotransferase, alanine aminotransferase (ALT), total bilirubin, alkaline phosphatase (ALP), gamma-glutamyl transpeptidase (γ GTP), white blood cell (WBC), platelets, and hemoglobin. Written informed consent was obtained from all patients or their guardians and provided to the Ethics Committee of the Graduate School of Kyoto University, Osaka City University and Ogaki Municipal Hospital, who approved this study in accordance with the Helsinki Declaration.

Treatment protocol

For all enrolled patients, treatment with PegIFN- α 2b (Schering-Plough Corporation, Kenilworth, NJ, USA) and ribavirin (Schering-Plough) was initiated at the beginning of the 1st week and lasted for 48 weeks. PegIFN was administered at a dose of 1.5 μ g/kg/week and ribavirin was administered at the dose recommended by the manufacturer.

Definition of drug response to therapy

The patients were classified into the following three groups at the completion of follow-up period (24 weeks): (1) sustained virological responder (SVR): a patient who was negative for serum HCV RNA during the 24 weeks following the completion of the

Table 5. Quality of NR-prediction by DLDA.

		Predicted		Total
		NR	nonNR(SVR+R)	
Diagnosed	NR	9	2	11
	nonNR(SVR+R)	4	28	32
Total		13	30	43

doi:10.1371/journal.pone.0019799.t005

Table 6. Result of the IL28B polymorphism (rs8099917).

		rs8099917		
		TT	TG	GG
outcome	NR	7	12	1
	Relapse	18	3	0
	SVR	30	1	0
	Total	55	16	1

doi:10.1371/journal.pone.0019799.t006

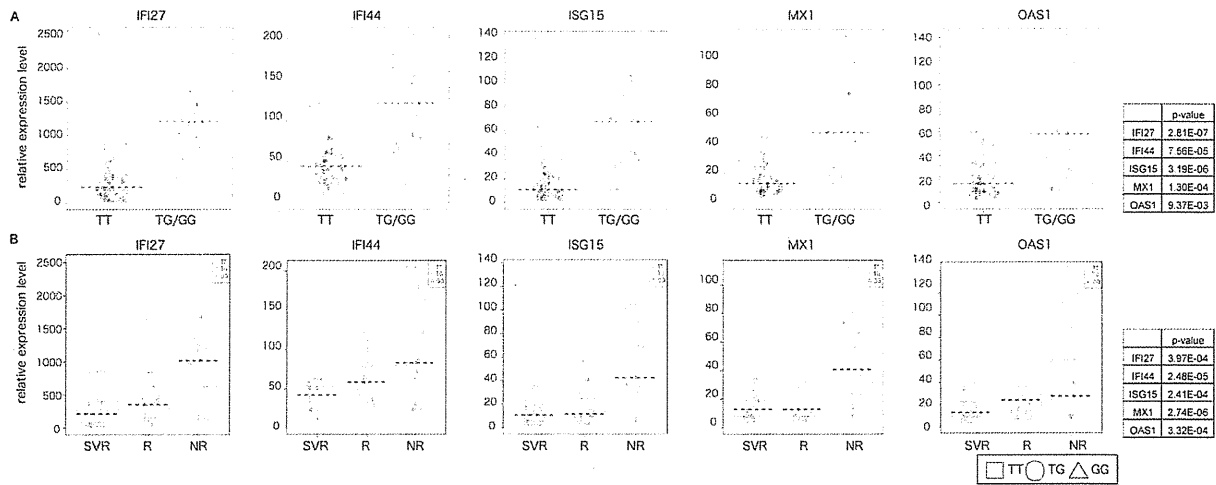


Figure 2. The relationship among the expression of IFN-related genes, IL28B polymorphism and clinical outcome. (A) The relationship between expression of ISG and five related genes (MX1, OAS1, ISG15, IFI27, and IFI44) in the liver of CH patients and IL28B with the major (TT) or minor (TG or GG) genotype (rs8099917) is shown. The p-value of the relationship between gene expression level and IL28B genotype is also depicted. (B) The relationship among the expression level of the above five genes, clinical outcome, and IL28B genotype in individual cases. Red square, green circle, and blue rectangle represent TT, TG, and GG in IL28B genotype, respectively. The p value was calculated from a linear regression employing outcome as an explanatory variable (in which SVR, R and NR are encoded to 0, 1 and 2 respectively) and expression level as the response variable. We tested the null hypothesis that the coefficient of the outcome is 0. Summary table of the p-value is also shown. NS shows no significant difference. doi:10.1371/journal.pone.0019799.g002

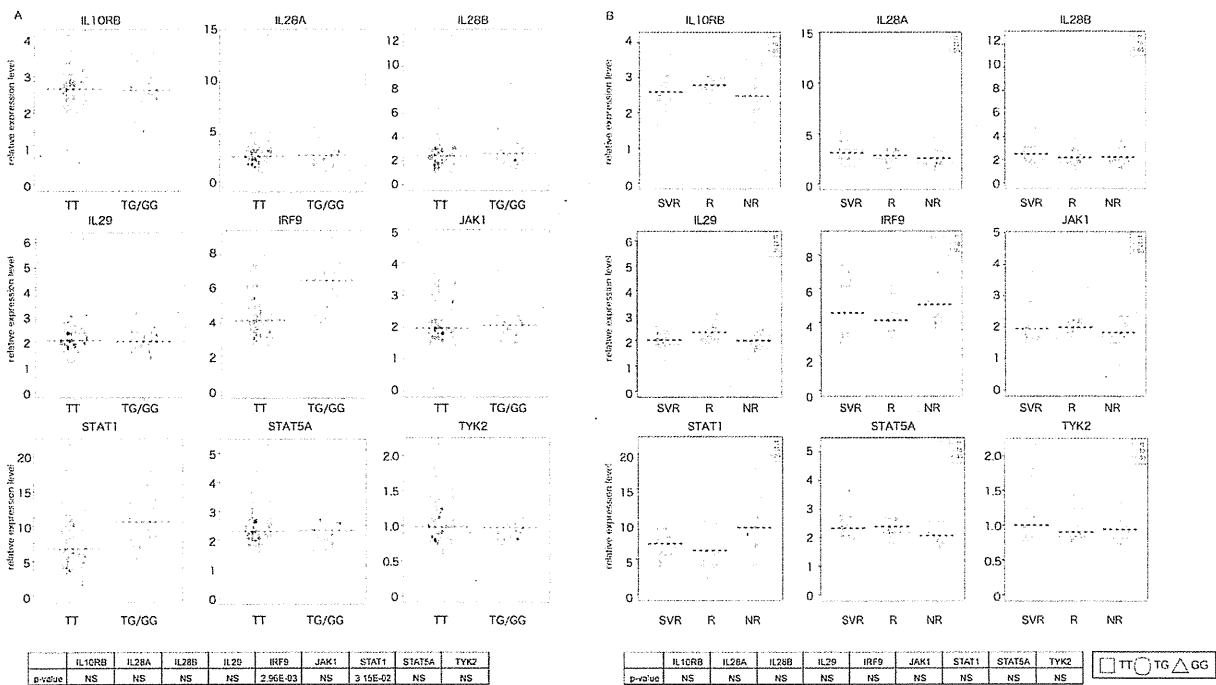


Figure 3. The relationship among the expression of IFN lambda-related genes, IL28B polymorphism and clinical outcome. (A) The relationship between the expression level of IFN lambda related genes (TYK2, STAT5A, STAT1, IL10RB, IL29, IL28A, IL28B, JAK1, and IRF9) in the liver of CH patients and IL28B with genotype. The p-value of the relationship between gene expression level and IL28B genotype is also presented. (B) The relationship among IFN lambda related genes, clinical outcome, and IL28B genotype in individual cases. Summary table of the p-value is also shown. NS was not significantly different. doi:10.1371/journal.pone.0019799.g003

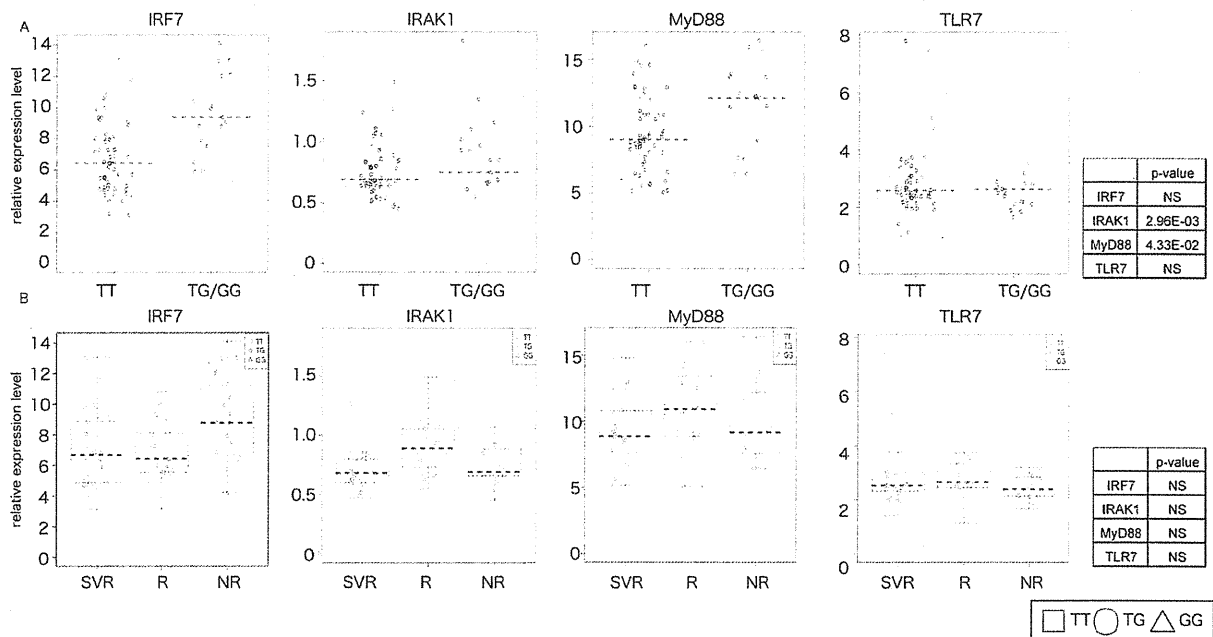


Figure 4. The relationship between the expression level of genes which participate in IFN production (TLR7, MyD88, IRAK1, and IRF7) in the liver of CH patients and IL28B genotype. (A) The relationship between IFN early response genes and clinical outcome is shown. A summary table of the p-value is also presented. NS shows no significant difference. (B) The relationship between IFN early response genes and IL28B genotype is shown. The p-value is also presented. doi:10.1371/journal.pone.0019799.g004

combination therapy; (2) relapse (R): a patient whose serum HCV RNA was negative by the end of the combination therapy but reappeared during the 24 week observation period; and (3) non responder (NR): a patient who was positive for serum HCV RNA during the entire course of the combination therapy (Figure 5). No patients were withdrawn from the study due to side effects or any other reason.

RNA preparation and real-time qPCR

Total RNA from tissue samples was prepared using a mirVana miRNA extraction Kit (Ambion, Austin, TX, USA) according to the manufacturer’s instruction. cDNA was synthesized by Transcriptor High Fidelity cDNA synthesis Kit (Roche, Basel, Switzerland). Total RNA (2 µg) in 11 µl of nuclease free water was added to 1 µl of 50 µM random hexamer and denatured for 10 min at 65°C. The denatured RNA mixture was added to 4 µl of 5x reverse transcriptase buffer, 2 µl of 10 mM dNTP, 0.5 µl of 40 U/ml RNase

inhibitor, and 0.5 µl of reverse transcriptase (FastStart Universal SYBR Green Master (Roche) in a total volume of 20 µl. cDNA synthesis was performed for 30 min at 50°C, and enzyme denaturation for 5 min at 85°C. Chromo 4 detector (Bio-Rad, Hercules, CA, USA) was used to detect mRNA expression. Assays were performed in triplicate, and the expression levels of target genes were normalized to that of the β-actin gene, as quantified using real-time qPCR as internal controls. Nucleotide sequences of primers were as follows: IFI27 (sense) 5'-ctagccacggaattaaccc-3', IFI27 (anti-sense) 5'-gactgcagatgaccacaag-3', IFI44 (sense) 5'-gcatgtaacgcattcaggctt-3', IFI44 (anti-sense) 5'-ccacaccagcgtttaccaac-3', ISG15 (sense) 5'-ctttgccaagtcaggagctt-3', ISG15 (anti-sense) 5'-gcccttgattctcaccaca-3', MX1 (sense) 5'-aatcagcctgctgacattgg-3', MX1 (anti-sense) 5'-gtgatgagctcgctgtaag-3', OAS1 (sense) 5'-gtgcgctcagctctgtactg-3', OAS1 (anti-sense) 5'-actaggcgatgaggctctt-3', and β-actin (sense) 5'-ccactggcatcgtgatggac-3', β-actin (anti-sense) 5'-ctattgccaatggatgacct-3'.

Table 7. Quality of NR-prediction by DLDA with IFN related gene and IL28B polymorphism A.IFN+IL28B.

		Predicted		Total
		NR	nonNR	
Diagnosed	NR	7	2	9
	nonNR	4	23	27
	Total	11	25	36

doi:10.1371/journal.pone.0019799.t007

Table 8. Quality of NR-prediction by DLDA with IFN related gene only.

		Predicted		Total
		NR	nonNR	
Diagnosed	NR	8	1	9
	nonNR	5	22	27
	Total	13	23	36

doi:10.1371/journal.pone.0019799.t008

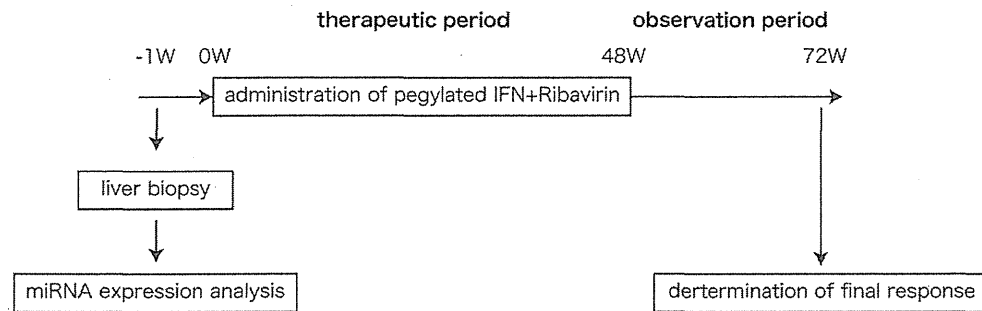


Figure 5. Study design and time line of response to combination therapy. The time frame of liver biopsy, microarray analysis, therapeutic period, observation period after combination therapy, and the judging of clinical outcome is shown.
doi:10.1371/journal.pone.0019799.g005

cDNA microarray

RNA was amplified and biotinylated using the MessageAmp-Biotin Enhanced Kit (Ambion). DNA oligonucleotide probes were synthesized onto a DNA microarray chip called Genopal (Mitsubishi Rayon) in order to detect the 237 genes (200 genes on Chip1 and 37 genes on Chip2) related to the innate immune response. Hybridization was carried out overnight at 65°C using Genopal in a hybridization buffer [0.12 M Tris-HCl/0.12 M NaCl/0.05% Tween-20]. After hybridization, Genopal was washed with hybridization buffer twice at 65°C for 20 min followed by washing in 0.12 M Tris-HCl/0.12 M NaCl at 65°C for 10 min. Genopal was then labeled with streptavidin-Cy5 (GE Healthcare Bioscience, Tokyo, Japan). The fluorescent labeled-Genopal was washed for 5 min four times with hybridization buffer at RT and scanned at multiple exposure times ranging from 0 to 40s by DNA microarray reader (Yokogawa Electric Co, Tokyo, Japan). Intensity values with the best exposure condition for each spot were selected. The data presented here have been deposited in NCBI's Gene Expression Omnibus and are accessible through GEO Series accession number GSE20119: <http://www.ncbi.nlm.nih.gov/geo/query/acc.cgi?token=xlmbxyumcwkeba&acc=GSE20119>. All data are MIAME compliant, and are also registered with GEO.

Statistical analysis

To identify the genes that varied significantly among NR, R, SVR and NL groups, one-way ANOVA and Turkey's post hoc tests were used to assess each of the 237 IFN related-genes on the arrays. Benjamini-Hochberg correction for multiple hypotheses testing was applied to all tests. P values <0.05 were considered statistically significant.

Method of predicting prognosis

The patients were randomly divided into two groups: one was used as a TS and the other VS to calculate the prediction discriminant. A prognosis signature (PS) was defined in terms of the expression levels of the six genes that differed significantly between NR and non-NR groups using post hoc analysis (IFI27,

IFI44, interferon-induced protein with tetratricopeptide repeats 3 (IFIT3), ISG15, MX1, OAS1). A prognosis predictor (PP) was computed by applying a diagonal linear DLDA to the TS [33] and then using it to predict the prognoses of the VS. The predicted and actual prognoses of VS patients were compared to obtain the following five measures of prognosis prediction performance: accuracy (proportion of correctly predicted prognoses), sensitivity (proportion of correctly predicted non-NR), specificity (proportion of correctly predicted NR), PPV (proportion of actual non-NR versus predicted non-NR) and NPV (proportion of actual NR versus predicted NR).

Genetic Variation of IL28B Polymorphism

Genotypes rs8099917 was determined in 72 out of 87 patients by Taqman SNP assays (Applied Biosystems) using a pre-designed and functionally tested probe (ABI assay ID (C_11710096_10)). The experiment was carried out according to the manufacturer's instruction.

Supporting Information

Figure S1 Real-time qPCR validation of the five IFN related genes. Each column represents the relative amount of mRNAs normalized to expression level of β -actin. The data shown are means+SD of three independent experiments. Asterisk was indicated to the significant difference at $p < 0.05$. (TIF)

Acknowledgments

The authors would like to thank Akihiro Tamori and Shouji Kubo of Osaka City University, for providing the liver samples taken from healthy patients.

Author Contributions

Conceived and designed the experiments: KS YM. Performed the experiments: KO SM T. Kawaguchi YM. Analyzed the data: T. Kawaguchi MT MK. Contributed reagents/materials/analysis tools: HT T. Kumada. Wrote the paper: HT KU T. Kawaguchi FM TF YM.

References

- Guidotti LG, Chisari FV (2006) Immunobiology and pathogenesis of viral hepatitis. *Annu Rev Pathol* 1: 23–61.
- Ikeda K, Arase Y, Saitoh S, Kobayashi M, Someya T, et al. (2006) Anticarcinogenic impact of interferon on patients with chronic hepatitis C: a large-scale long-term study in a single center. *Intervirology* 49: 82–90.
- Fried MW, Shiffman ML, Reddy KR, Smith C, Marinos G, et al. (2002) Peginterferon alfa-2a plus ribavirin for chronic hepatitis C virus infection. *N Engl J Med* 347: 975–982.
- Accola MA, Huang B, Al Masri A, McNiven MA (2002) The antiviral dynamin family member, MxA, tubulates lipids and localizes to the smooth endoplasmic reticulum. *J Biol Chem* 277: 21829–21835.
- Malathi K, Dong B, Gale M, Jr., Silverman RH (2007) Small self-RNA generated by RNase L amplifies antiviral innate immunity. *Nature* 448: 816–819.
- Akuta N, Suzuki F, Kawamura Y, Yatsuji H, Sezaki H, et al. (2007) Predictive factors of early and sustained responses to peginterferon plus ribavirin

- combination therapy in Japanese patients infected with hepatitis C virus genotype 1b: amino acid substitutions in the core region and low-density lipoprotein cholesterol levels. *J Hepatol* 46: 403–410.
7. Enomoto N, Sakuma I, Asahina Y, Kurosaki M, Murakami T, et al. (1996) Mutations in the nonstructural protein 5A gene and response to interferon in patients with chronic hepatitis C virus 1b infection. *N Engl J Med* 334: 77–81.
 8. Bondini S, Younossi ZM (2006) Non-alcoholic fatty liver disease and hepatitis C infection. *Minerva Gastroenterol Dietol* 52: 135–143.
 9. Sharma P, Marrero JA, Fontana RJ, Greenson JK, Conjeevaram H, et al. (2007) Sustained virologic response to therapy of recurrent hepatitis C after liver transplantation is related to early virologic response and dose adherence. *Liver Transpl* 13: 1100–1108.
 10. Murakami Y, Tanaka M, Toyoda H, Hayashi K, Kuroda M, et al. (2010) Hepatic microRNA expression is associated with the response to interferon treatment of chronic hepatitis C. *BMC Med Genomics* 3: 48.
 11. Tanaka Y, Nishida N, Sugiyama M, Kurosaki M, Matsuura K, et al. (2009) Genome-wide association of IL28B with response to pegylated interferon-alpha and ribavirin therapy for chronic hepatitis C. *Nat Genet* 41: 1105–1109.
 12. Suppiah V, Moldovan M, Ahlenstiel G, Berg T, Weltman M, et al. (2009) IL28B is associated with response to chronic hepatitis C interferon-alpha and ribavirin therapy. *Nat Genet* 41: 1100–1104.
 13. Ge D, Fellay J, Thompson AJ, Simon JS, Shianna KV, et al. (2009) Genetic variation in IL28B predicts hepatitis C treatment-induced viral clearance. *Nature* 461: 399–401.
 14. Szabo G, Chang S, Dolganiuc A (2007) Altered innate immunity in chronic hepatitis C infection: cause or effect? *Hepatology* 46: 1279–1290.
 15. Conry SJ, Milkovich KA, Yonkers NL, Rodriguez B, Bernstein HB, et al. (2009) Impaired plasmacytoid dendritic cell (PDC)-NK cell activity in viremic human immunodeficiency virus infection attributable to impairments in both PDC and NK cell function. *J Virol* 83: 11175–11187.
 16. Pulendran B, Tang H, Denning TL (2008) Division of labor, plasticity, and crosstalk between dendritic cell subsets. *Curr Opin Immunol* 20: 61–67.
 17. Wertheimer AM, Bakke A, Rosen HR (2004) Direct enumeration and functional assessment of circulating dendritic cells in patients with liver disease. *Hepatology* 40: 335–345.
 18. Mengshol JA, Golden-Mason L, Castelblanco N, Im KA, Dillon SM, et al. (2009) Impaired plasmacytoid dendritic cell maturation and differential chemotaxis in chronic hepatitis C virus: associations with antiviral treatment outcomes. *Gut* 58: 964–973.
 19. Patzwahl R, Meier V, Ramadori G, Mihm S (2001) Enhanced expression of interferon-regulated genes in the liver of patients with chronic hepatitis C virus infection: detection by suppression-subtractive hybridization. *J Virol* 75: 1332–1338.
 20. Sarasin-Filipowicz M (2010) Interferon therapy of hepatitis C: molecular insights into success and failure. *Swiss Med Wkly* 140: 3–11.
 21. Uno K, Sugimoto Y, Kakimi K, Moriyasu F, Hirotsuki M, et al. (2005) Impairment of IFN-alpha production capacity in patients with hepatitis C virus and the risk of the development of hepatocellular carcinoma. *World J Gastroenterol* 11: 7330–7334.
 22. Critchley-Thorne RJ, Simons DL, Yan N, Miyahira AK, Dirbas FM, et al. (2009) Impaired interferon signaling is a common immune defect in human cancer. *Proc Natl Acad Sci U S A* 106: 9010–9015.
 23. Sarasin-Filipowicz M, Oakeley EJ, Duong FH, Christen V, Terracciano L, et al. (2008) Interferon signaling and treatment outcome in chronic hepatitis C. *Proc Natl Acad Sci U S A* 105: 7034–7039.
 24. Asselah T, Bieche I, Narguet S, Sabbagh A, Laurendeau I, et al. (2008) Liver gene expression signature to predict response to pegylated interferon plus ribavirin combination therapy in patients with chronic hepatitis C. *Gut* 57: 516–524.
 25. Feld JJ, Nanda S, Huang Y, Chen W, Cam M, et al. (2007) Hepatic gene expression during treatment with peginterferon and ribavirin: Identifying molecular pathways for treatment response. *Hepatology* 46: 1548–1563.
 26. Chen L, Borozan I, Feld J, Sun J, Tannis LL, et al. (2005) Hepatic gene expression discriminates responders and nonresponders in treatment of chronic hepatitis C viral infection. *Gastroenterology* 128: 1437–1444.
 27. Chen L, Borozan I, Sun J, Guindi M, Fischer S, et al. (2010) Cell-type specific gene expression signature in liver underlies response to interferon therapy in chronic hepatitis C infection. *Gastroenterology* 138: 1123–1133 e1121–1123.
 28. Okumura A, Lu G, Pitha-Rowe I, Pitha PM (2006) Innate antiviral response targets HIV-1 release by the induction of ubiquitin-like protein ISG15. *Proc Natl Acad Sci U S A* 103: 1440–1445.
 29. Chen TY, Hsieh YS, Wu TT, Yang SF, Wu CJ, et al. (2007) Impact of serum levels and gene polymorphism of cytokines on chronic hepatitis C infection. *Transl Res* 150: 116–121.
 30. Younossi ZM, Baranova A, Afendy A, Collantes R, Stepanova M, et al. (2009) Early gene expression profiles of patients with chronic hepatitis C treated with pegylated interferon-alfa and ribavirin. *Hepatology* 49: 763–774.
 31. Dill MT, Duong FH, Vogt JE, Bibert S, Bochud PY, et al. (2011) Interferon-Induced Gene Expression is a Stronger Predictor of Treatment Response Than IL28B Genotype in Patients With Hepatitis C. *Gastroenterology*.
 32. Honda M, Sakai A, Yamashita T, Nakamoto Y, Mizukoshi E, et al. (2010) Hepatic ISG expression is associated with genetic variation in interleukin 28B and the outcome of IFN therapy for chronic hepatitis C. *Gastroenterology* 139: 499–509.
 33. Bair E, Tibshirani R (2004) Semi-supervised methods to predict patient survival from gene expression data. *PLoS Biol* 2: E108.

Retinoic Acid-Inducible Gene-I-Like Receptors

Kazuhide Onoguchi, Mitsutoshi Yoneyama, and Takashi Fujita

Retinoic acid-inducible gene-I (RIG-I), melanoma differentiation-associated 5 (MDA5), and laboratory of genetics and physiology 2 (LGP2) form a family of DExD/H box RNA helicases. RIG-I-like receptors (RLRs) are expressed ubiquitously at low levels, and their expression is induced by treatment with type I interferon (IFN) or a viral infection. RLRs function as sensors for the detection of viral RNA (such as double-stranded RNA) in the cytoplasm to initiate antiviral responses by producing type I and type III IFNs. Unlike Toll-like receptors, which sense exogenous pathogen-associated molecular patterns, RLRs detect cytoplasmic viral RNA. Because RLRs are IFN-inducible viral sensors, they are critical in amplifying antiviral responses.

Retinoic Acid-Inducible Gene-I-Like Receptor as Interferon Stimulated Genes

ALTHOUGH RETINOIC ACID-INDUCIBLE GENE-I (RIG)-like receptor (RLRs) are detectable in all tissues, treatment with type I interferon (IFN) induces their expression at the mRNA and protein level (Kang and others 2004; Yoneyama and others 2004, 2005). Viral infections induce RLR expression in type I IFN receptor-deficient cells, suggesting the existence of a direct mechanism. This is consistent with the observation that such cells efficiently produce IFN in response to a viral infection (Yoneyama and others 1998). Similar to protein kinase RNA-dependent (PKR) and oligoadenylate synthetase (OAS), whose enzymatic activities require dsRNA, RLR also requires agonist RNA for signaling to initiate IFN production (see below). However, unlike PKR and OAS, no direct role of RLR in inhibiting viral replication has been reported.

Structure of RLRs

The function of RIG-I was discovered by screening an expression cDNA library (Yoneyama and others 2004). The cDNA clone initially obtained encoded the N-terminal portion of RIG-I. This partial clone encompassed the signaling domain with 2 repeats of the Caspase activation and recruitment domain (CARD, Fig. 1). Forced expression of the N-terminal portion resulted in the activation of type I IFN genes without any viral infection. However, the full-length protein exhibits little activity, suggesting autorepression. The largest portion of RIG-I is the helicase domain containing helicase motifs conserved in other DExH/D helicases. The C-terminal region consists of a single structural domain termed the RNA recognition domain because this portion is responsible for binding dsRNA (Cui and others 2008;

Takahashi and others 2008). The repression function was mapped to a region partially overlapping the RNA-binding domain (Saito and others 2007). MDA5 contains these 3 domains; however, its RNA recognition domain exhibits significantly low affinity for dsRNA as well as little repression (Saito and others 2007; Takahashi and others 2009). Laboratory of genetics and physiology 2 (LGP2) lacks the N-terminal tandem CARD but retains the RNA-binding and repressive functions (Yoneyama and others 2005; Komuro and Horvath 2006; Takahashi and others 2009).

RLR as the Cytoplasmic Sensor for Viral Infections

An antiviral function of RLR was identified by the generation of knockout mice. RIG-I-deficient mice and cells exhibited impaired IFN production in response to different viruses (Table 1) (Kato and others 2005, 2006). However, RIG-I deficiency had little influence on infections of *Picornaviridae* (Kato and others 2006). MDA5 appeared to be critical for sensing this family to produce IFN, suggesting that retention of these nonredundant has physiological significance (Gitlin and others 2006; Kato and others 2006). As expected, infections of some viruses are sensed by both RIG-I and MDA5 (Fredericksen and others 2008; Kato and others 2008; Loo and others 2008). Further, DNA viruses activate IFN genes through the activation of RIG-I or MDA5, presumably sensing RNA species produced during viral replication (Ablasser and others 2009; Chiu and others 2009; Choi and others 2009). *Legionella pneumophila*, a bacterium that replicates intracellularly, induces IFN production through the activation of RIG-I (Monroe and others 2009).

LGP2, which lacks a signaling domain, blocks the IFN production induced by viral infections when overexpressed (Rothenfusser and others 2005; Yoneyama and others

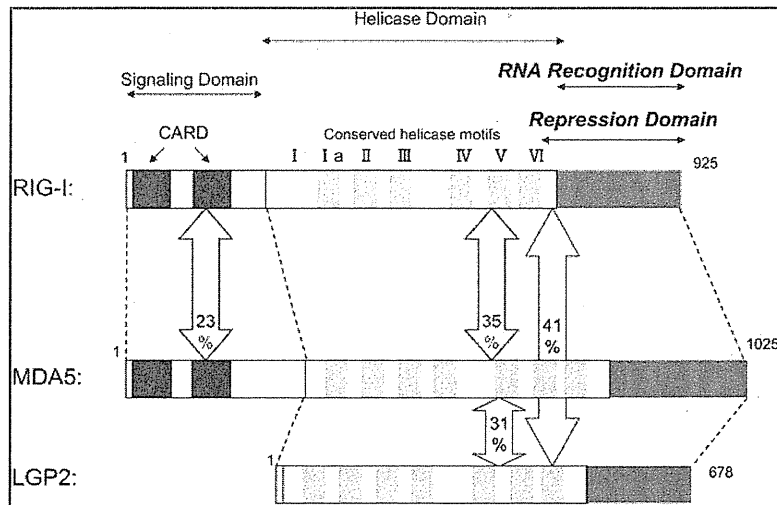


FIG. 1. Structure of RLRs. Schematic representation of RLR domains. The Caspase activation and recruitment domain (CARD), Helicase domain, and RNA recognition domain are indicated. Conserved helicase motifs (I to VI) are shown. The repression domain (hRIG-I: aa. 735–925; hLGP2: aa. 476–678) and RNA recognition domain (hRIG-I: aa. 799–925; hMDA5: aa. 896–1,025; hLGP2: aa. 546–678) are shown. Conservation of the amino acid sequence in the indicated region among human RLRs is indicated in percentage terms. RIG-I, retinoic acid inducible gene-I; MDA5, melanoma differentiation-associated 5; LGP, laboratory of genetics and physiology; RLR, RIG-I-like receptor.

2005). However, LGP2-knockout mice or cells exhibited diminished IFN production upon EMCV infection, suggesting functional cooperation between LGP2 and MDA5 (Venkataraman and others 2007; Satoh and others 2010). Upon infection by VSV, LGP2-deficient dendritic cells exhibited

reduced IFN production (Satoh and others 2010); however, a different knockout line exhibited the opposite effect (Venkataraman and others 2007). This could be due to a different virus strain (Indiana strain wild-type VS M protein mutant) or cell type (fibroblast VS cDC). LGP2 deficiency did not

TABLE 1. VIRUS-SPECIFIC RECOGNITION BY RETINOIC ACID-INDUCIBLE GENE-I-LIKE RECEPTORS

Family	Genome	Type species	RLR	Reference
Picornaviridae	(+)ssRNA	Encephalomyocarditis virus	MDA5	Kato and others (2006), Gitlin and others (2006)
		Theiler's virus		
		Mengo virus		
Caliciviridae		Murine norovirus-1	MDA5/RIG-1	McCartney and others (2008)
Coronaviridae		Murine hepatitis virus		Roth-Cross and others (2008)
Flaviviridae		West Nile virus		Fredericksen and others (2008)
		Dengue virus	Loo and others (2008)	
		Japanese encephalitis virus	Kato and others (2006)	
		Hepatitis C virus	Saito and others (2008)	
Orthomyxoviridae		(-)ssRNA	Influenza A virus	RIG-I
Paramyxoviridae	Newcastle disease virus		Kato and others (2006)	
	Sendai virus		Kato and others (2006)	
Rhabdoviridae	Vesicular stomatitis virus		Kato and others (2006)	
Reoviridae	dsRNA	Reovirus	MDA5/RIG-1	Kato and others (2008), Loo and others (2008)
Poxviridae	dsDNA	Vaccinia virus	MDA5	Pichlmair and others (2009)
		Myxoma virus	RIG-I	Wang and others (2008)
Herpesviridae		Epstein-Barr virus	RIG-I	Samanta and others (2006)
Summary of the specificity with which RLRs recognize a variety of viruses. Family and type of genomic nucleic acids are indicated.				

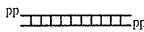
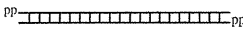
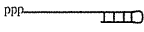
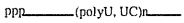
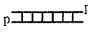
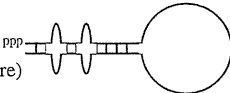
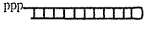
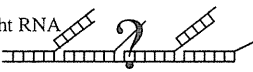
RNA	structure	RLR	reference
Short poly I:C (~300 bp)		RIG-I	Kato and others 2008
Long poly I:C (> 4 kbp)		MDA5	Kato and others 2008
in vitro T7 transcript (with copyback)		RIG-I	Schlee and others 2009 Schmidt and others 2009
HCV RNA		RIG-I	Saito and others 2008
RNaseL cleavage product (RNA of host/virus)		RIG-I (MDA5)	Malathi and others 2007
Viral genomic RNA (with panhandle structure)		RIG-I	Rehwinkel and others 2010
RNA of DI particle (copyback)		Unidentified	Strahle and others 2006
High molecular weight RNA (RNA web)		MDA5	Pichlmair and others 2009

FIG. 2. Viral RNA patterns and RLR recognition. Synthetic and viral RNA patterns and the RLRs recognizing them are summarized. The schematic structure of each RNA pattern is indicated. The precise structure of RNA web is unknown.

influence the IFN production triggered by an influenza A virus infection (Satoh and others 2010), suggesting that LGP2 also functions in a virus-specific manner.

The viral specificity described above is determined by RNA species produced by different viruses and/or inhibitory molecules encoded by different viruses (below). Figure 2 summarizes the relationship between the structure of RNA and the sensors. Commercial poly I:C activates MDA5 but not RIG-I (Kato and others 2006). Double-stranded RNA produced by annealing complementary T7 transcripts preferentially activates RIG-I (Kato and others 2006). The length of dsRNA is one of the determinants for this specificity: short (~300bp) and long (>4kbp) poly I:C activate RIG-I and MDA5, respectively (Kato and others 2008). Although it was reported that 5'-ppp-containing single-stranded RNA is the ligand for RIG-I (Hornung and others 2006; Pichlmair and others 2006), later it was discovered that RNA produced by *in vitro* transcription contains a partial double-stranded structure due to copyback activity of the phage polymerase (Schlee and others 2009; Schmidt and others 2009). Importantly, chemically synthesized single-stranded RNA with 5'-ppp is inactive toward RIG-I. It is proposed that RIG-I

recognizes most efficiently 5'-ppp-containing RNA with a partial double-stranded structure (Schlee and others 2009). Natural RNA of this category includes viral genomic panhandle RNA such as of influenza A virus (Rehwinkel and others 2010) and copyback RNA contained in defective interfering (DI) particles of Sendai virus (Strahle and others 2006). Mapping of HCV RNA revealed that a poly (rU) tract is responsible for activating RIG-I (Saito and others 2008). In this case, 5'-ppp is indispensable. It is implied that host RNaseL activated by the antiviral response participates in producing the RLR ligand (dsRNA with 3' monophosphate) by digesting host or viral RNA (Malathi and others 2007). EMCV and Vaccinia virus produce high molecular RNA (RNA web) with a single- and double-stranded structure, and this RNA complex is responsible for the activation of MDA5 (Pichlmair and others 2009); however, the molecular mechanism by which MDA5 but not RIG-I recognizes this complex is unknown.

Viral Countermeasures for RLR-Mediated Signaling

Viruses have acquired inhibitory molecules to block antiviral responses and secure their survival. Often nonstructural,

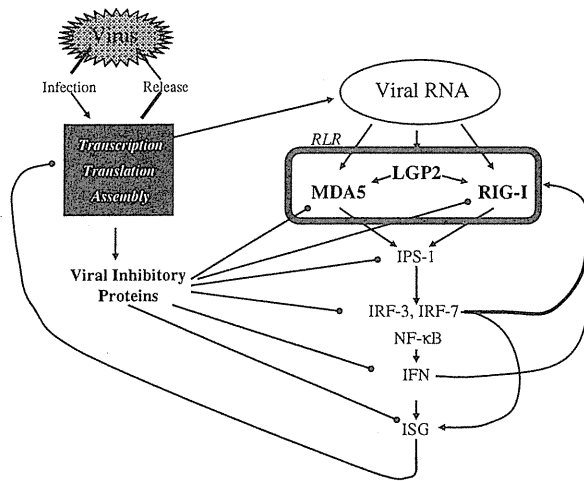


FIG. 3. RLR-mediated signaling and its regulation. Viral replication and viral RNA-induced innate immune signaling are summarized (see text). IPS-1, interferon promoter stimulator 1; ISG, interferon stimulated gene.

accessory proteins confer such activities. NS-1 of the influenza A virus inhibits production of IFN by blocking RIG-I's function (Guo and others 2007; Opitz and others 2007). The NS3/4A complex of the hepatitis C virus inactivates interferon promoter stimulator 1 (IPS-1), an immediate downstream signaling adaptor of RIG-I, through serine protease activity (Li and others 2005). The V protein of *Paramyxoviridae* selectively blocks MDA5 (Andrejeva and others 2004). In addition, replication-competent viruses have acquired means to counteract the host immune system, and the specificity of the inhibitors also contributes to the virus specificity of RLR.

Targets of RLR Signaling and Signal Amplification Mediated by RLR

As mentioned, RLR requires agonist RNA to trigger signals, which result in the activation of several classes of genes. The first category is the genes activated by viral infection or dsRNA transfection, but not by IFN treatment. Genes of this group include those of type I and type III IFN (Onoguchi and others 2007). The second category is the genes secondarily activated by secreted IFN. Genes of this category are activated with delayed kinetics and dependent on functional IFN receptors (Sadler and Williams 2008). The third category is the genes activated by both virus and RNA as well as by the secreted IFN (Mossman and others 2001).

Figure 3 summarizes viral replication and signal amplification mediated by RLRs. The infection initiates transcription of the viral genome within the cells. Eventually, viral structural and nonstructural proteins are translated and accumulate. The viral genome and structural proteins assemble to form new virions to expand the infection. Viral RNA with unusual structures such as those described in Fig. 2 are recognized by RLR, resulting in the signal to produce type I and type III IFN. The signal directly activates some of the interferon stimulated genes (ISGs) and the secreted IFN secondarily activates other ISGs to establish an antiviral state. Because RLRs are ISGs, the signaling is amplified. However, viruses encode inhibitory proteins to counteract the compo-

nents of the IFN signaling system, and the initial balance between viral replication and host antiviral response determines the outcome of the infection.

Author Disclosure Statement

No competing financial interests exist.

References

- Ablasser A, Bauernfeind F, Hartmann G, Latz E, Fitzgerald KA, Hornung V. 2009. RIG-I-dependent sensing of poly(dA:dT) through the induction of an RNA polymerase III-transcribed RNA intermediate. *Nat Immunol* 10(10):1065–1072.
- Andrejeva J, Childs KS, Young DF, Carlos TS, Stock N, Goodbourn S, Randall RE. 2004. The V proteins of paramyxoviruses bind the IFN-inducible RNA helicase, mda-5, and inhibit its activation of the IFN-beta promoter. *Proc Natl Acad Sci U S A* 101(49):17264–17269.
- Chiu YH, Macmillan JB, Chen ZJ. 2009. RNA polymerase III detects cytosolic DNA and induces type I interferons through the RIG-I pathway. *Cell* 138(3):576–591.
- Choi MK, Wang Z, Ban T, Yanai H, Lu Y, Koshiba R, Nakaima Y, Hangai S, Savitsky D, Nakasato M, Negishi H, Takeuchi O, Honda K, Akira S, Tamura T, Taniguchi T. 2009. A selective contribution of the RIG-I-like receptor pathway to type I interferon responses activated by cytosolic DNA. *Proc Natl Acad Sci U S A* 106(42):17870–17875.
- Cui S, Eisenacher K, Kirchhofer A, Brzozka K, Lammens A, Lammens K, Fujita T, Conzelmann KK, Krug A, Hopfner KP. 2008. The C-terminal regulatory domain is the RNA 5'-triphosphate sensor of RIG-I. *Mol Cell* 29(2):169–179.
- Fredericksen BL, Keller BC, Fornek J, Katze MG, Gale M, Jr. 2008. Establishment and maintenance of the innate antiviral response to West Nile virus involves both RIG-I and MDA5 signaling through IPS-1. *J Virol* 82(2):609–616.
- Gitlin L, Barchet W, Gilfillan S, Cella M, Beutler B, Flavell RA, Diamond MS, Colonna M. 2006. Essential role of mda-5 in type I IFN responses to polyriboinosinic:polyribocytidylic acid and encephalomyocarditis picornavirus. *Proc Natl Acad Sci U S A* 103(22):8459–8464.
- Guo Z, Chen LM, Zeng H, Gomez JA, Plowden J, Fujita T, Katz JM, Donis RO, Sambhara S. 2007. NS1 Protein of Influenza A virus inhibits the function of intracytoplasmic pathogen sensor, RIG-I. *Am J Respir Cell Mol Biol* 36:263–269.
- Hornung V, Ellegast J, Kim S, Brzozka K, Jung A, Kato H, Poeck H, Akira S, Conzelmann KK, Schlee M, Endres S, Hartmann G. 2006. 5'-Triphosphate RNA is the ligand for RIG-I. *Science* 314(5801):994–997.
- Kang DC, Gopalkrishnan RV, Lin L, Randolph A, Valerie K, Pestka S, Fisher PB. 2004. Expression analysis and genomic characterization of human melanoma differentiation associated gene-5, mda-5: a novel type I interferon-responsive apoptosis-inducing gene. *Oncogene* 23(9):1789–1800.
- Kato H, Sato S, Yoneyama M, Yamamoto M, Uematsu S, Matsui K, Tsujimura T, Takeda K, Fujita T, Takeuchi O, Akira S. 2005. Cell type-specific involvement of RIG-I in antiviral response. *Immunity* 23(1):19–28.
- Kato H, Takeuchi O, Mikamo-Satoh E, Hirai R, Kawai T, Matsushita K, Hiiragi A, Dermody TS, Fujita T, Akira S. 2008. Length-dependent recognition of double-stranded ribonucleic acids by retinoic acid-inducible gene-I and melanoma differentiation-associated gene 5. *J Exp Med* 205(7):1601–1610.
- Kato H, Takeuchi O, Sato S, Yoneyama M, Yamamoto M, Matsui K, Uematsu S, Jung A, Kawai T, Ishii KJ, Yamaguchi O, Otsu K, Tsujimura T, Koh CS, Reis e Sousa C, Matsuura Y, Fujita T,

- Akira S. 2006. Differential roles of MDA5 and RIG-I helicases in the recognition of RNA viruses. *Nature* 441(7089):101–105.
- Komuro A, Horvath CM. 2006. RNA- and virus-independent inhibition of antiviral signaling by RNA helicase LGP2. *J Virol* 80(24):12332–12342.
- Li XD, Sun L, Seth RB, Pineda G, Chen ZJ. 2005. Hepatitis C virus protease NS3/4A cleaves mitochondrial antiviral signaling protein off the mitochondria to evade innate immunity. *Proc Natl Acad Sci U S A* 102(49):17717–17722.
- Loo YM, Fornek J, Crochet N, Bajwa G, Perwitasari O, Martinez-Sobrido L, Akira S, Gill MA, Garcia-Sastre A, Katze MG, Gale M, Jr. 2008. Distinct RIG-I and MDA5 signaling by RNA viruses in innate immunity. *J Virol* 82(1):335–345.
- Malathi K, Dong B, Gale M, Jr., Silverman RH. 2007. Small self-RNA generated by RNase L amplifies antiviral innate immunity. *Nature* 448(7155):816–819.
- McCartney SA, Thackray LB, Gitlin L, Gilfillan S, Virgin HW, Colonna M. 2008. MDA-5 recognition of a murine norovirus. *PLoS Pathog* 4(7):e1000108.
- Monroe KM, McWhirter SM, Vance RE. 2009. Identification of host cytosolic sensors and bacterial factors regulating the type I interferon response to *Legionella pneumophila*. *PLoS Pathog* 5(11):e1000665.
- Mossman KL, Macgregor PF, Rozmus JJ, Goryachev AB, Edwards AM, Smiley JR. 2001. Herpes simplex virus triggers and then disarms a host antiviral response. *J Virol* 75(2):750–758.
- Onoguchi K, Yoneyama M, Takemura A, Akira S, Taniguchi T, Namiki H, Fujita T. 2007. Viral infections activate types I and III interferon genes through a common mechanism. *J Biol Chem* 282(10):7576–7581.
- Opitz B, Rejaibi A, Dauber B, Eckhard J, Vinzing M, Schneck B, Hippenstiel S, Suttrop N, Wolff T. 2007. IFN β induction by influenza A virus is mediated by RIG-I which is regulated by the viral NS1 protein. *Cell Microbiol* 9:930–938.
- Pichlmair A, Schulz O, Tan CP, Naslund TI, Liljestrom P, Weber F, Reis e Sousa C. 2006. RIG-I-mediated antiviral responses to single-stranded RNA bearing 5'-phosphates. *Science* 314(5801):997–1001.
- Pichlmair A, Schulz O, Tan CP, Rehwinkel J, Kato H, Takeuchi O, Akira S, Way M, Schiavo G, Reis e Sousa C. 2009. Activation of MDA5 requires higher-order RNA structures generated during virus infection. *J Virol* 83(20):10761–10769.
- Rehwinkel J, Tan CP, Goubau D, Schulz O, Pichlmair A, Bier K, Robb N, Vreede F, Barclay W, Fodor E, Reis e Sousa C. 2010. RIG-I detects viral genomic RNA during negative-strand RNA virus infection. *Cell* 140(3):397–408.
- Roth-Cross JK, Bender SJ, Weiss SR. 2008. Murine coronavirus mouse hepatitis virus is recognized by MDA5 and induces type I interferon in brain macrophages/microglia. *J Virol* 82(20):9829–9838.
- Rothenfusser S, Goutagny N, DiPerna G, Gong M, Monks BG, Schoenemeyer A, Yamamoto M, Akira S, Fitzgerald KA. 2005. The RNA helicase Lgp2 inhibits TLR-independent sensing of viral replication by retinoic acid-inducible gene-I. *J Immunol* 175(8):5260–5268.
- Sadler AJ, Williams BR. 2008. Interferon-inducible antiviral effectors. *Nat Rev Immunol* 8(7):559–568.
- Saito T, Hirai R, Loo YM, Owen D, Johnson CL, Sinha SC, Akira S, Fujita T, Gale M, Jr. 2007. Regulation of innate antiviral defenses through a shared repressor domain in RIG-I and LGP2. *Proc Natl Acad Sci U S A* 104(2):582–587.
- Saito T, Owen DM, Jiang F, Marcotrigiano J, Gale M, Jr. 2008. Innate immunity induced by composition-dependent RIG-I recognition of hepatitis C virus RNA. *Nature* 454(7203):523–527.
- Samanta M, Iwakiri D, Kanda T, Imaizumi T, Takada K. 2006. EB virus-encoded RNAs are recognized by RIG-I and activate signaling to induce type I IFN. *EMBO J* 25(18):4207–4214.
- Satoh T, Kato H, Kumagai Y, Yoneyama M, Sato S, Matsushita K, Tsujimura T, Fujita T, Akira S, Takeuchi O. 2010. LGP2 is a positive regulator of RIG-I- and MDA5-mediated antiviral responses. *Proc Natl Acad Sci U S A* 107(4):1512–1517.
- Schlee M, Roth A, Hornung V, Hagmann CA, Wimmenauer V, Barchet W, Coch C, Janke M, Mihailovic A, Wardle G, Juraneck S, Kato H, Kawai T, Poeck H, Fitzgerald KA, Takeuchi O, Akira S, Tuschl T, Latz E, Ludwig J, Hartmann G. 2009. Recognition of 5' triphosphate by RIG-I helicase requires short blunt double-stranded RNA as contained in panhandle of negative-strand virus. *Immunity* 31(1):25–34.
- Schmidt A, Schwerdt T, Hamun W, Hellmuth JC, Cui S, Wenzel M, Hoffmann FS, Michallet MC, Besch R, Hopfner KP, Endres S, Rothenfusser S. 2009. 5'-Triphosphate RNA requires base-paired structures to activate antiviral signaling via RIG-I. *Proc Natl Acad Sci U S A* 106(29):12067–12072.
- Strahle L, Garcin D, Kolakofsky D. 2006. Sendai virus defective-interfering genomes and the activation of interferon-beta. *Virology* 351(1):101–111.
- Takahasi K, Kumeta H, Tsuduki N, Narita R, Shigemoto T, Hirai R, Yoneyama M, Horiuchi M, Ogura K, Fujita T, Inagaki F. 2009. Solution structures of cytosolic RNA sensor MDA5 and LGP2 C-terminal domains: identification of the RNA recognition loop in RIG-I-like receptors. *J Biol Chem* 284(26):17465–17474.
- Takahasi K, Yoneyama M, Nishihori T, Hirai R, Kumeta H, Narita R, Gale M, Jr., Inagaki F, Fujita T. 2008. Nonspecific RNA-sensing mechanism of RIG-I helicase and activation of antiviral immune responses. *Mol Cell* 29(4):428–440.
- Venkataraman T, Valdes M, Elsy R, Kakuta S, Caceres G, Saijo S, Iwakura Y, Barber GN. 2007. Loss of DExD/H box RNA helicase LGP2 manifests disparate antiviral responses. *J Immunol* 178(10):6444–6455.
- Wang F, Gao X, Barrett JW, Shao Q, Bartee E, Mohamed MR, Rahman M, Werden S, Irvine T, Cao J, Dekaban GA, McFadden G. 2008. RIG-I mediates the co-induction of tumor necrosis factor and type I interferon elicited by myxoma virus in primary human macrophages. *PLoS Pathog* 4(7):e1000099.
- Yoneyama M, Kikuchi M, Matsumoto K, Imaizumi T, Miyagishi M, Taira K, Foy E, Loo YM, Gale M, Jr., Akira S, Yonehara S, Kato A, Fujita T. 2005. Shared and unique functions of the DExD/H-Box helicases RIG-I, MDA5, and LGP2 in antiviral innate immunity. *J Immunol* 175(5):2851–2858.
- Yoneyama M, Kikuchi M, Natsukawa T, Shinobu N, Imaizumi T, Miyagishi M, Taira K, Akira S, Fujita T. 2004. The RNA helicase RIG-I has an essential function in double-stranded RNA-induced innate antiviral responses. *Nat Immunol* 5(7):730–737.
- Yoneyama M, Suhara W, Fukuhara Y, Fukuda M, Nishida E, Fujita T. 1998. Direct triggering of the type I interferon system by virus infection: activation of a transcription factor complex containing IRF-3 and CBP/p300. *EMBO J* 17(4):1087–1095.

Address correspondence to:

Takashi Fujita, Ph.D.

Department of Molecular Genetics

Institute for Virus Research

Kyoto University

53 Shogoin-Kawara Sakyo

Kyoto 606-8507

Japan

E-mail: tfujita@virus.kyoto-u.ac.jp

Received 3 August 2010/Accepted 3 August 2010

Hiroki Kato
Kiyohiro Takahasi
Takashi Fujita

RIG-I-like receptors: cytoplasmic sensors for non-self RNA

Authors' addresses

Hiroki Kato^{1,2}, Kiyohiro Takahasi^{1,3}, Takashi Fujita^{1,2}

¹Laboratory of Molecular Genetics, Institute for Virus Research, Kyoto University, Kyoto, Japan.

²Laboratory of Molecular Cell Biology, Graduate School of Biostudies, Kyoto University, Kyoto, Japan.

³Institute for Innovative NanoBio Drug Discovery and Development, Graduate School of Pharmaceutical Sciences, Kyoto University, Kyoto, Japan.

Correspondence to:

Takashi Fujita

Laboratory of Molecular Genetics

Institute for Virus Research, Kyoto University

Shogoinkawahara-cho, Sakyo-ku

Kyoto 606-8507

Japan

Tel.: +81 75 751 4031

Fax: +81 75 751 4031

e-mail: tfujita@virus.kyoto-u.ac.jp

Acknowledgement

The authors have no conflicts of interest to declare.

Summary: Viral infection results in the generation of non-self RNA species in the cells, which is recognized by retinoic acid inducible gene-I-like receptors (RLRs), and initiates innate antiviral responses, including the production of proinflammatory cytokines and type I interferon. In this review, we summarize reports on virus-specificity of RLRs, structures of non-self RNA patterns, structural biology of RLRs, and the signaling adapter molecules involved in antiviral innate immunity.

Keywords: antiviral innate immunity, type I interferon, RIG-I-like receptors, non-self RNA

RIG-I-like receptors (RLRs)

Pattern recognition receptors (PRRs) are essential in innate immunity. Major PRRs are Toll-like receptors (TLRs), retinoic acid inducible gene-I (RIG-I)-like receptors (RLRs), and nucleotide oligomerization domain (Nod)-like receptors (NLRs) (1–3). TLR3, TLR7, TLR8, and TLR9 detect viral nucleic acids in endosome (4–8). These receptors essentially sense extracellular molecules incorporated into endosome by endocytosis. These sensors detect viral nucleic acids, released from virus-infected cells, and activate subsequent immune reactions. RLRs detect replicating viruses in cytoplasm, particularly at early phase of viral infection. Some of the NLRs sense viral infection to initiate inflammatory responses. Activation of innate immune responses lead to the induction of type I and III interferon (IFN) and inflammatory cytokines, whose antiviral activity blocks viral replication and facilitate the activation of antigen-presenting cells to activate antigen-specific immunity to eradicate the viral pathogens.

RLRs include RIG-I, MDA5, and LGP2, all of which contain a DExD/H box helicase domain (9, 10). The helicase domain retains catalytic activity to unwind double stranded RNA (dsRNA) in an adenosine triphosphate (ATP) hydrolysis-dependent

manner (11); however, unwinding *per se* may not be inducing antiviral activity. RIG-I and MDA5 contain tandem caspase recruitment and activation domain (CARD) at their amino-termini. Forced overexpression of the CARD alone is sufficient to drive antiviral signaling resulting in IFN production, showing that this domain is responsible for signaling. Indeed, the CARD of RIG-I interacts with another CARD-containing molecule, interferon- β promoter stimulator 1 (IPS-1) (also termed as MAVS, VISA, and Cardif) (12–15). Overexpression of full-length RIG-I exhibits low basal activity. Furthermore, although IFN treatment strongly induces RIG-I protein, IFN treatment alone does not activate IFN genes. Thus, an autorepression model has been proposed. It was demonstrated that a region of RIG-I acts as repression domain, which functions in *cis* as well as *trans*. LGP2 also retains repression domain; however, the corresponding region of MDA5 does not exhibit repression function. The C-terminus of RLRs consists of a domain [C-terminal domain (CTD)] and is responsible for binding with dsRNA. It has been hypothesized that binding of viral RNA with RIG-I induces conformational change in the presence of ATP to unmask CARD, but no report has experimentally demonstrated the conformational change so far.

Recognition of RNA viruses by RLRs

Based on the gene-targeting studies, it has been revealed that RLRs are essential for the production of type I IFNs and proinflammatory cytokines, such as interleukin-6 (IL-6), in response to viral infection. Double knockout cells for RIG-I and MDA5 produce no significant IFN upon viral infection, showing that these receptors are essential for sensing cytoplasmic viral RNA (16).

Cells lacking RIG-I are defective in producing type I IFNs and inflammatory cytokines in response to various RNA viruses including Newcastle disease virus (NDV) (*Paramyxoviridae*), Sendai virus (SeV) (*Paramyxoviridae*), vesicular stomatitis virus (VSV) (*Rhabdoviridae*), influenza A virus (*Orthomyxoviridae*), or Japanese encephalitis virus (JEV) (*Flaviviridae*), while MDA5-deficient cells respond normally to these viruses (16, 17). In contrast, the production of IFN in response to several picornaviruses, including encephalomyocarditis virus (EMCV), Mengo virus, and Theiler's virus, is abrogated in MDA5-deficient cells but not in cells lacking RIG-I (17, 18). Murine norovirus-1 (*Caliciviridae*) and murine hepatitis virus (*Coronaviridae*) are recognized by MDA5 (19, 20). In addition to JEV, another flavivirus, hepatitis C virus (HCV) is also recognized by RIG-I, while both RIG-I and MDA5 likely recognize Den-

gue virus and West Nile virus (*Flavivirus*), redundantly (21–23). A vaccine strain of measles virus (*Paramyxoviridae*) activates IFN through the activation of both RIG-I and MDA5, whereas the wildtype measles virus fails to induce type I IFN production (24). Reovirus, whose genome consists of segmented dsRNA, induces IFN production mainly through MDA5 with minor contribution from RIG-I (25).

Overexpression of LGP2, which lacks CARD, resulted in diminished IFN production by virus (10). However, LGP2 knockout cells exhibited attenuated IFN production upon infection of VSV or EMCV (26), suggesting that LGP2 cooperates with either RIG-I or MDA5 to sense viral RNA under physiological conditions. Influenza A virus-induced IFN production was normal in LGP2-deficient cells, suggesting that LGP2 specifically senses particular RNA patterns.

A DNA virus, Epstein–Barr virus (EBV), is reported to produce small RNAs that induce RIG-I-mediated IFN responses (27). Another DNA virus, herpes simplex virus (HSV), is also reported to activate both RIG-I- and MDA5-dependent IFN responses via dsRNA produced during its replication (28).

RNA ligands of RLRs

Polyriboinosinic:polyribocytidylic acid

Polyriboinosinic:polyribocytidylic acid (polyI:C), a synthetic dsRNA, which was selected as a potent non-viral IFN inducer, acts as a ligand for TLR3 and RLRs (4, 25). Although the mechanism underlying is not known, poly I:C exhibits highest activity among the possible combinations of RNA homopolymer duplexes. Poly I:C is generated by annealing poly I and poly C, which are synthesized by polynucleotide phosphorylase. This enzyme catalyzes the polymerization of nucleotide diphosphate, thus poly I:C harbors a 5'-diphosphate (29).

Two groups demonstrated that MDA5 is essential for poly I:C-mediated IFN production by gene targeting (16, 18). The specificity originates from the length of dsRNA rather than base composition (25). Commercial poly I:C runs as dsRNA of 4–8 kbp in gel electrophoresis. Partial digestion of the poly I:C with a dsRNA specific endonuclease, RNaseIII, led to the generation of trimmed poly I:C of about 300 bp. This short poly I:C activates RIG-I. Interestingly, short poly I:C fails to activate MDA5, and long poly I:C is incapable of activating RIG-I, although both of these bind to long and short poly I:C. Therefore, both RIG-I and MDA5 are necessary to sense various length of dsRNA. The precise mechanism of size discrimination by RIG-I and MDA5 is not known.

5' tri-phosphate RNAs

RNA transcribed from DNA template by T7 RNA polymerase is a strong inducer of type I IFN (30). Further studies revealed that 5'-triphosphate containing RNA, such as genomes of most RNA viruses, and *in vitro* transcripts are selectively recognized by RIG-I (31, 32). Since the 5'-triphosphate moieties of most host transcripts are removed by adding 7-methyl-guanosine cap (in the case of mRNA) or by processing (tRNA and rRNA), these self-RNAs are refractory to detection by RIG-I. However more recently, it was revealed that 5'-triphosphate *per se* is not sufficient for RIG-I activation. This is consistent with observations that dsRNA without 5'-triphosphate can be recognized by RIG-I particularly for long dsRNA. Therefore, dsRNA structure is prerequisite for RIG-I activation and 5'-triphosphate facilitates the recognition of short dsRNA. In addition, removal of 5'-triphosphate is a viral strategy to avoid recognition by RIG-I. A viral peptide, VPg, is covalently attached to the 5' end of Picornaviridae RNA, thus lacking 5'-triphosphate (33). Hantaan virus (HTNV), Crimean-Congo hemorrhagic fever virus (CCHFV) (Bunyaviridae), and Borna disease virus (BDV) (Bornaviridae) do not trigger RIG-I-mediated IFN responses, because the 5'-triphosphate structure of these viral genomic RNA is removed by processing (34).

Transfection of AT-rich dsDNA (typically a synthetic polydAdT:polydAdT) results in the type I IFN induction (35). It was revealed that polydAdT:polydAdT is transcribed by host DNA-dependent RNA polymerase III and that the resultant 5'-triphosphate dsRNA is detected by RIG-I (36, 37). The polymerase III-mediated mechanism may explain IFN induction by some DNA viruses or intracellular bacteria.

Nallagatla et al. (38) suggested that the 5' tri-phosphate signature is sensed by protein kinase R (PKR) in addition to dsRNA. Further studies are required to elucidate the mechanism by which the 5' tri-phosphate signature activates both RIG-I and PKR and to understand its biological significance.

Viral RNA ligand for RLR

Garcin's group (39) nicely showed this dsRNA-dependent activation of RIG-I, using a SeV infection. They generated SeV expressing GFP mRNA or antisense GFP mRNA and performed co-infection of two types of SeV. They found that the resulting capped dsRNA of GFP sequences induced an IFN response that was dependent on RIG-I. In addition to engineered SeV, natural VSV, a ssRNA virus recognized by RIG-I, was shown to produce dsRNA in infected cells (25). Induction of IFNs by

RNAs from VSV-infected cells was impaired by disrupting dsRNA, suggesting the presence of dsRNA in VSV-infected cells is important for RIG-I mediated IFN responses. The fragments produced by VSV were about 2–2.5 kbp much shorter than the length of the 11 kb VSV genomic RNA, suggesting that these dsRNA were not derived from replication intermediates of VSV. Rather, the dsRNA maybe be derived from defective interfering (DI) particles, whose snap-back dsRNAs are reported to be about 2.2 kbp, generated in VSV-infected cells, although the viral dsRNA signature recognized by RIG-I remains to be further characterized. Recently, panhandle structure of the influenza virus genome is also reported as RIG-I ligand (40). It is of interest to clarify which ligand is the major source of RIG-I-dependent IFN production in individual viral infection.

IFN production induced by long segments purified from the reovirus genome (about 3.9 kbp) is impaired in MDA5-deficient cells (25). Further, the very large RNA species (stuck at the top of the gel during electrophoresis) generated by EMCV or vaccinia virus infection is a specific ligand for MDA5 (41). Although the precise structure of the RNA (termed RNA web), is not known, a highly ordered structure is critical for this activity, as heat treatment inactivated the complex.

RNaseL-cleaved RNA

RNaseL is an endonuclease thought to cleave viral RNA. Silverman's group (42) showed that RNaseL-deficient cells showed attenuated induction of IFN in response to poly I:C or Sendai virus. In addition, in the infection with EMCV and Sendai virus, RNaseL-deficient mice showed impaired IFN production in sera. The RNaseL cleavage products activate RIG-I and MDA5, leading to production of type I IFNs. This mechanism potentially generates RLR ligands from self-RNA as well as viral RNA.

Poly-U/UC rich RNA

Infection with HCV is known to be regulated by hepatic immune defense triggered by RIG-I. Mapping of the HCV genome for RIG-I activation revealed that 5'-triphosphate signature was necessary but not sufficient for the activation of RIG-I and that a polyuridine motif (poly-U/UC-rich region) at the 3'-non-translated region is critical for efficient activation of RIG-I (43). They extended their finding and found that 5'-triphosphate genomic poly-U/A-rich RNA motifs within the rabies virus leader sequence, Ebola virus 3' region, and measles virus leader sequence were also important for RIG-I

activation (43). However, GC-rich RNA motifs failed to induce the signaling (43). Thus, A/U composition and poly-U motifs are possible determinants of viral RNA recognition by antiviral innate immunity. Representative RNA patterns and recognizing RLRs are summarized in Fig. 1.

Structure of RLRs

Two groups independently identified the RNA recognition domain that is located to the C-terminus to the helicase domain CTD. Takahashi et al. (11) showed that RIG-I CTD specifically binds dsRNA and 5'-triphosphate RNA and solved its solution structure. Furthermore, these studies revealed that large positive charged surface that locates the center of the structure is the RNA binding site by NMR titration (11). Cui et al. also identified the domain and solved the crystal structure (44). The structures of MDA5 and LGP2 CTDs were also solved and their structural features are very similar to RIG-I CTD (45). Recent studies have solved the crystal structures of RIG-I CTD bound to both blunt ended double-strand RNA and dsRNA with 5'-triphosphate (46–48). Both CTD structures showed that the same basic surface revealed in previous studies was essential for the RNA recognition. However, two different ended RNAs bound RIG-I CTD in different orientations (46–48). The complex structure of LGP2 bound to the blunt end of dsRNA was also solved by x-ray crystallography, but the orientation of the RNA in the complex was also different from the RNAs bound to the RIG-I CTD (49). The biological

significance of these co-crystals requires further investigation because the biological activity of the RNA used for crystal is not well investigated, particularly the presence or absence of 5'-triphosphate. These observations imply that RIG-I specifically recognizes the end structure of viral RNA, especially blunt end dsRNA or 5'-triphosphate structure. However, it has been controversial if end structure affects recognition by RIG-I (11, 45, 46). In addition, AFM analysis suggests that RIG-I aggregates around the short poly I:C, excluding the possibility of end-specific binding (25). For certain, better understanding of the activation of the RIG-I/RNA complex awaits further structural elucidation of inactive (free RIG-I in closed structure) and activated (RIG-I/RNA complex in the presence of ATP) complexes.

RLR signaling and its regulation

Upon binding to viral RNA in the presence of ATP, RIG-I changes its conformation to expose the CARD. The activated RIG-I forms oligomer, which allows the CARDS of RIG-I to interact with a CARD-containing adapter, IPS-1, which is localized on the outer membrane of the mitochondrion. MDA5 also transduces signaling via IPS-1. IPS-1 subsequently activates two I κ B kinase (IKK)-related kinases, IKK-i, and TANK-binding kinase 1 (TBK1) via tumor necrosis factor (TNF) receptor-associated factor 3 (TRAF3) (50–52). These kinases phosphorylate IRF3 and IRF7, resulting in their




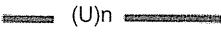




RNA pattern	Structure	RLR	Ref.
A Long polyI:C	5'PP  PP5'	MDA5	25, 16,18
B Short polyI:C (short dsRNA without 5' triphosphates)		RIG-I	25
C 5' triphosphate RNAs (generated by T7 polymerase)	5'PPP 	RIG-I	31,32
D poly U/UC rich RNA (HCV)	5'PPP  (U) _n 	RIG-I	43
E Panhandle region of Influenzavirus genome		RIG-I	40
F RNaseL-cleaved self RNAs	3'p  p3'	RIG-I MDA5	42
G RNA web (higher order structure)		MDA5	41

Fig. 1. RNA patterns and their recognition by RLRs. Summary of synthetic and viral RNA patterns and the RLRs recognizing them.

translocation from the cytoplasm into the nucleus, which activates transcription of genes encoding type I IFNs and IFN-inducible genes (53, 54). In addition, IPS-1 activates NF- κ B via a FADD and caspase-8/10 pathway to regulate the expression of proinflammatory cytokine genes (55).

Many molecules have been reported to modulate the RLR-mediated signaling pathway (described above) through direct interaction with RLRs or with signaling molecules. For instance, Src homology 2 (SH2) domain-containing phosphatase-1 (SHP-1) is reported to activate RIG-I-mediated signaling by binding directly to RIG-I (56). Dihydroacetone kinase (DAK) was identified as a MDA5-interacting protein and was shown to negatively regulate MDA5 (57). NLRX1 (also known as NOD9) is localized to the mitochondrial outer membranes and is suggested to function as a negative regulator of IPS-1 via a direct interaction (58). Suppressor of IKK ϵ (SIKE) forms a complex with TBK1/IKK ϵ and inhibits the interaction of RIG-I or IRFs with TBK1/IKK ϵ in the basal condition, while viral infection leads to dissociation of SIKE from TBK/IKK ϵ (59). Molecules involved in the autophagic machinery, Atg5-atg12, are reported to inhibit the interaction

between RIG-I and IPS-1 by association with the CARD of RIG-I and with IPS-1 (60). Recent studies from two independent groups (61, 62) identified the same signal-modulator molecule, designated as stimulator of IFN genes (STING), also called mediator of IRF-3 activation (MITA). STING is reported to localize to the endoplasmic reticulum (ER) membrane, and STING interacts with RIG-I (but not MDA5), and SSR2/TRP β complex, required for protein translocation across the ER membrane. The other group reported that STING is expressed on the outer membrane of mitochondrion, where it interacts directly with IPS-1 and IRF-3 and positively regulates the virus-dependent recruitment of TBK1 to the IPS-1 complex on mitochondrion.

Ubiquitination of RLRs is reported to control their signals both positively and negatively. The CARDs of RIG-I undergo Lys63-linked ubiquitination by tripartite motif 25 (TRIM 25), and this ubiquitination is necessary for efficient activation of RIG-I mediated signaling (63). Interestingly, MDA5 does not undergo ubiquitination by TRIM25, suggesting that CARDs of RIG-I and MDA5 are differentially regulated. A tumor suppressor, CYLD (cylindromatosis), is reported to negatively regulate

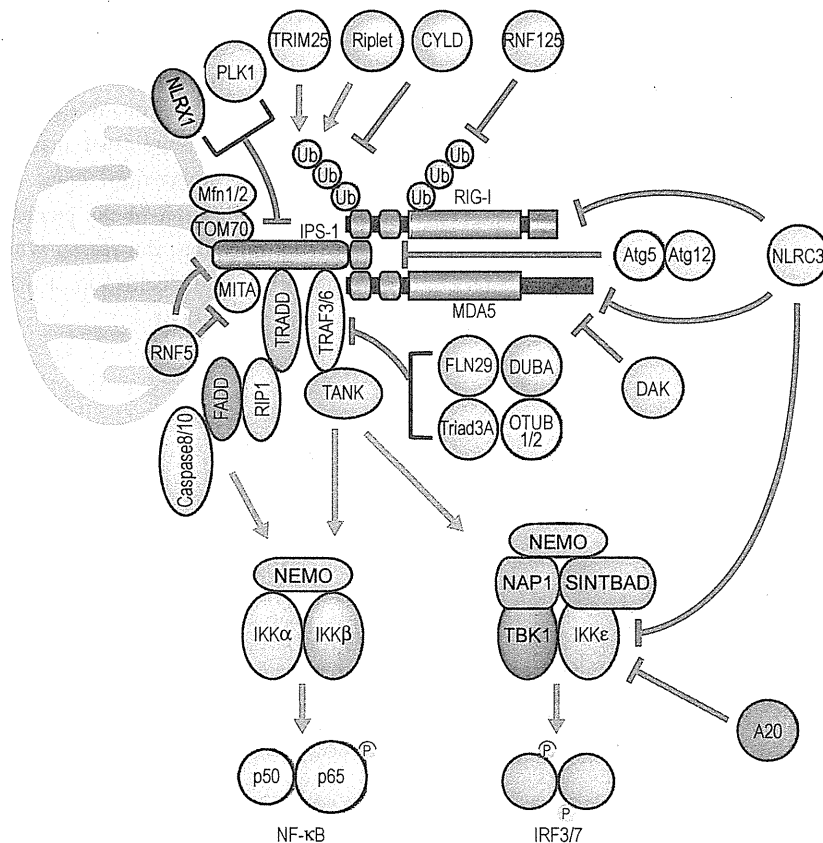


Fig. 2. RLR-mediated signaling and adapter molecules. Positive and negative regulation is indicated by red and blue lines, respectively.

the RIG-I-mediated signaling by deubiquitinating the TRIM25-mediated ubiquitination of RIG-I (64). Another E3 ubiquitin ligase RNF135/Riplet is shown to promote Lys63-linked ubiquitination of the C-terminal region of RIG-I, which results in activation of IFN promoter (65). RIG-I also undergoes Lys48-linked polyubiquitination by the E3 ubiquitin ligase RNF125, leading to its proteasomal degradation, which inhibits aberrant activation of RIG-I mediated signaling. Further, RNF125 conjugates ubiquitin to MDA5 as well as IPS-1, which results in suppressing the functions of these proteins (66). It was also recently shown that REUL is an E3 ubiquitin ligase of RIG-I and specifically stimulates RIG-I-mediated IFN signaling (67). The Lys 154, 164, and 172 residues of the RIG-I CARD domain are critical for efficient REUL-mediated ubiquitination, as well as the ability of RIG-I to induce activation of the IFN- β promoter. ISGylation also modulates RLR-signaling. RIG-I is ISGylated by the ubiquitin-like protein, ISG15, which regulates the activity of RNF125 together with UbcH8, an E2 ubiquitin-conjugating enzyme (68). UbcH8 suppresses ubiquitination of RIG-I by RNF125, and the suppression by UbcH8 is relieved by ISG15.

Artificial aggregation of IPS-1 in the cytoplasm is sufficient for activation of antiviral signaling (69), suggesting that the activity of IPS-1 is regulated by its oligomerization induced by physical interaction of CARD of RIG-I or MDA5. Interestingly, IPS-1 aggregation is observed in cells stably expressing Flag-tagged IPS-1 upon infection by various viruses or 5'-triphosphate RNA. Normally IPS-1 is localized on the outer membrane of the mitochondrion, which may restrict its movement. The IPS-1 aggregation requires mitofusin 1, a mitochondrial regulator for its fusion (70). Mitofusin 1 is also reported to be critical for mitochondrial elongation

induced by certain strains of Sendai virus. These results suggest that the activity of IPS-1 requires dynamic fission and fusion of mitochondrion to facilitate efficient signaling by its oligomerization. However, there are contradictory reports on the function of mitochondrion and mitofusins (71). The adaptor molecules involved in RLR-mediated signaling are summarized in Fig. 2.

In addition to host regulatory factors mentioned above, viruses acquire means to evade antiviral immunity of the host. Modification of viral RNA and assembly of nucleocapsid are major strategies to escape from detection by RLRs. Viral non-structural (NS) proteins often participate in the counteraction of antiviral cascades. A large number of viral inhibitory proteins have been identified that block RLR signaling at various levels (reviewed in 72, 73).

Conclusions and perspectives

Cumulative studies based on RLR knockout mice/cells and various viruses revealed the mechanism by which RLRs sense viral invasion as well as viral strategies to evade antiviral responses mediated by RLRs. As described in this review, it is clear that RIG-I and MDA5 are essential sensors for RNA viruses and that these helicases discriminate self and non-self RNAs by precise recognition of virus-specific RNA signatures. However, elucidation of many signaling regulators has made the picture more complicated than previously appreciated. Certainly, many interesting topics remain to be clarified, including identification of the precise RNA ligands of RLRs during viral infection, the reason why IPS-1 localizes to the mitochondrion, and elucidation of the molecular structure of inactive and active RIG-I.

References

1. Takeuchi O, Akira S. Pattern recognition receptors and inflammation. *Cell* 2010;140:805–820.
2. Fujita T. A nonself RNA pattern: tri-p to pan-handle. *Immunity* 2009;31:4–5.
3. Beutler B, et al. Genetic analysis of resistance to viral infection. *Nat Rev Immunol* 2007;7:753–766.
4. Alexopoulou L, Holt AC, Medzhitov R, Flavell RA. Recognition of double-stranded RNA and activation of NF- κ B by Toll-like receptor 3. *Nature* 2001;413:732–738.
5. Heil F, et al. Species-specific recognition of single-stranded RNA via toll-like receptor 7 and 8. *Science* 2004;303:1526–1529.
6. Diebold SS, Kaisho T, Hemmi H, Akira S, Reis e Sousa C. Innate antiviral responses by means of TLR7-mediated recognition of single-stranded RNA. *Science* 2004;303:1529–1531.
7. Hemmi H, et al. Small anti-viral compounds activate immune cells via the TLR7 MyD88-dependent signaling pathway. *Nat Immunol* 2002;3:196–200.
8. Hemmi H, et al. A Toll-like receptor recognizes bacterial DNA. *Nature* 2000;408:740–745.
9. Yoneyama M, et al. The RNA helicase RIG-I has an essential function in double-stranded RNA-induced innate antiviral responses. *Nat Immunol* 2004;5:730–737.
10. Yoneyama M, et al. Shared and unique functions of the DExD/H-box helicases RIG-I, MDA5, and LGP2 in antiviral innate immunity. *J Immunol* 2005;175:2851–2858.
11. Takahashi K, et al. Nonself RNA-sensing mechanism of RIG-I helicase and activation of antiviral immune responses. *Mol Cell* 2008;29:428–440.
12. Kawai T, et al. IPS-1, an adaptor triggering RIG-I- and Mda5-mediated type I interferon induction. *Nat Immunol* 2005;6:981–988.
13. Xu LG, Wang YY, Han KJ, Li LY, Zhai Z, Shu HB. VISA is an adapter protein required for virus-triggered IFN- β signaling. *Mol Cell* 2005;19:727–740.

14. Seth RB, Sun L, Ea CK, Chen ZJ. Identification and characterization of MAVS, a mitochondrial antiviral signaling protein that activates NF- κ B and IRF 3. *Cell* 2005;122:669–682.
15. Meylan E, et al. Cardif is an adaptor protein in the RIG-I antiviral pathway and is targeted by hepatitis C virus. *Nature* 2005;437:1167–1172.
16. Kato H, et al. Differential roles of MDA5 and RIG-I helicases in the recognition of RNA viruses. *Nature* 2006;441:101–105.
17. Kato H, et al. Cell type-specific involvement of RIG-I in antiviral response. *Immunity* 2005;23:19–28.
18. Gitlin L, et al. Essential role of mda-5 in type I IFN responses to polyriboinosinic: polyribocytidylic acid and encephalomyocarditis picornavirus. *Proc Natl Acad Sci USA* 2006;103:8459–8464.
19. McCartney SA, Thackray LB, Gitlin L, Gilfillan S, Virgin HW, Colonna M. MDA-5 recognition of a murine norovirus. *PLoS Pathog* 2008;4:e1000108.
20. Roth-Cross JK, Bender SJ, Weiss SR. Murine coronavirus mouse hepatitis virus is recognized by MDA5 and induces type I interferon in brain macrophages/microglia. *J Virol* 2008;82:9829–9838.
21. Foy E, et al. Control of antiviral defenses through hepatitis C virus disruption of retinoic acid-inducible gene-I signaling. *Proc Natl Acad Sci USA* 2005;102:2986–2991.
22. Loo YM, et al. Distinct RIG-I and MDA5 signaling by RNA viruses in innate immunity. *J Virol* 2008;82:335–345.
23. Fredericksen BL, Gale M Jr. West Nile virus evades activation of interferon regulatory factor 3 through RIG-I-dependent and -independent pathways without antagonizing host defense signaling. *J Virol* 2006;80:2913–2923.
24. Shingai M, et al. Differential type I IFN-inducing abilities of wild-type versus vaccine strains of measles virus. *J Immunol* 2007;179:6123–6133.
25. Kato H, et al. Length-dependent recognition of double-stranded ribonucleic acids by retinoic acid-inducible gene-I and melanoma differentiation-associated gene 5. *J Exp Med* 2008;205:1601–1610.
26. Satoh T, et al. LGP2 is a positive regulator of RIG-I- and MDA5-mediated antiviral responses. *Proc Natl Acad Sci USA* 2010;107:1512–1517.
27. Samanta M, Iwakiri D, Kanda T, Imaizumi T, Takada K. EB virus-encoded RNAs are recognized by RIG-I and activate signaling to induce type I IFN. *EMBO J* 2006;25:4207–4214.
28. Rasmussen SB, et al. Herpes simplex virus infection is sensed by both Toll-like receptors and retinoic acid-inducible gene-like receptors, which synergize to induce type I interferon production. *J Gen Virol* 2009;90:74–78.
29. Grunberg-Manago M, Oritz PJ, Ochoa S. Enzymatic synthesis of nucleic acidlike polynucleotides. *Science* 1955;122:907–910.
30. Kim DH, Longo M, Han Y, Lundberg P, Cantin E, Rossi JJ. Interferon induction by siRNAs and ssRNAs synthesized by phage polymerase. *Nat Biotechnol* 2004;22:321–325.
31. Hornung V, et al. 5'-Triphosphate RNA is the ligand for RIG-I. *Science* 2006;314:994–997.
32. Pichlmair A, et al. RIG-I-mediated antiviral responses to single-stranded RNA bearing 5'-phosphates. *Science* 2006;314:997–1001.
33. Pallansch MA, Kew OM, Palmenberg AC, Golini F, Wimmer E, Rueckert RR. Picornaviral VPg sequences are contained in the replicase precursor. *J Virol* 1980;35:414–419.
34. Habjan M, et al. Processing of genome 5' termini as a strategy of negative-strand RNA viruses to avoid RIG-I-dependent interferon induction. *PLoS ONE* 2008;3:e2032.
35. Ishii KJ, et al. A Toll-like receptor-independent antiviral response induced by double-stranded B-form DNA. *Nat Immunol* 2006;7:40–48.
36. Ablasser A, Bauernfeind F, Hartmann G, Latz E, Fitzgerald KA, Hornung V. RIG-I-dependent sensing of poly(dA:dT) through the induction of an RNA polymerase III-transcribed RNA intermediate. *Nat Immunol* 2009;10:1065–1072.
37. Chiu YH, MacMillan JB, Chen ZJ. RNA polymerase III detects cytosolic DNA and induces type I interferons through the RIG-I pathway. *Cell* 2009;138:576–591.
38. Nallagatla SR, Hwang J, Toroney R, Zheng X, Cameron CE, Bevilacqua PC. 5'-triphosphate-dependent activation of PKR by RNAs with short stem-loops. *Science* 2007;318:1455–1458.
39. Hausmann S, Marq JB, Tapparel C, Kolakofsky D, Garcin D. RIG-I and dsRNA-induced IFN β activation. *PLoS ONE* 2008;3:e3965.
40. Rehwinkel J, et al. RIG-I detects viral genomic RNA during negative-strand RNA virus infection. *Cell* 2010;140:397–408.
41. Pichlmair A, et al. Activation of MDA5 requires higher-order RNA structures generated during virus infection. *J Virol* 2009;83:10761–10769.
42. Malathi K, Dong B, Gale M Jr, Silverman RH. Small self-RNA generated by RNase L amplifies antiviral innate immunity. *Nature* 2007;448:816–819.
43. Saito T, Owen DM, Jiang F, Marcotrigiano J, Gale M Jr. Innate immunity induced by composition-dependent RIG-I recognition of hepatitis C virus RNA. *Nature* 2008;454:523–527.
44. Cui S, et al. The C-terminal regulatory domain is the RNA 5'-triphosphate sensor of RIG-I. *Mol Cell* 2008;29:169–179.
45. Takahashi K, et al. Solution structures of cytosolic RNA sensor MDA5 and LGP2 C-terminal domains: identification of the RNA recognition loop in RIG-I-like receptors. *J Biol Chem* 2009;284:17465–17474.
46. Lu C, et al. The structural basis of 5' triphosphate double-stranded RNA recognition by RIG-I C-terminal domain. *Structure* 2010;18:1032–1043.
47. Wang Y, et al. Structural and functional insights into 5'-ppp RNA pattern recognition by the innate immune receptor RIG-I. *Nat Struct Mol Biol* 2010;17:781–787.
48. Lu C, Ranjith-Kumar CT, Hao L, Kao CC, Li P. Crystal structure of RIG-I C-terminal domain bound to blunt-ended double-strand RNA without 5' triphosphate. *Nucleic Acids Res* 2011;39:1565–1575.
49. Li X, et al. The RIG-I-like receptor LGP2 recognizes the termini of double-stranded RNA. *J Biol Chem* 2009;284:13881–13891.
50. Fitzgerald KA, et al. IKKepsilon and TBK1 are essential components of the IRF3 signaling pathway. *Nat Immunol* 2003;4:491–496.
51. Hemmi H, et al. The roles of two I κ B kinase-related kinases in lipopolysaccharide and double stranded RNA signaling and viral infection. *J Exp Med* 2004;199:1641–50.
52. Häcker H, et al. Specificity in Toll-like receptor signalling through distinct effector functions of TRAF3 and TRAF6. *Nature* 2006;439:204–207.
53. Sato M, et al. Distinct and essential roles of transcription factors IRF-3 and IRF-7 in response to viruses for IFN- α / β gene induction. *Immunity* 2000;13:539–548.
54. Honda K, et al. IRF-7 is the master regulator of type-I interferon-dependent immune responses. *Nature* 2005;434:772–777.
55. Takahashi K, Kawai T, Kumar H, Sato S, Yonehara S, Akira S. Roles of caspase-8 and caspase-10 in innate immune responses to double-stranded RNA. *J Immunol* 2006;176:4520–4524.
56. An H, et al. Phosphatase SHP-1 promotes TLR- and RIG-I-activated production of type I interferon by inhibiting the kinase IRAK1. *Nat Immunol* 2008;9:542–550.
57. Diao F, et al. Negative regulation of MDA5-but not RIG-I-mediated innate antiviral signaling by the dihydroxyacetone kinase. *Proc Natl Acad Sci USA* 2007;104:11706–11.
58. Moore CB, et al. NLRX1 is a regulator of mitochondrial antiviral immunity. *Nature* 2008;451:573–577.
59. Huang J, Liu T, Xu LG, Chen D, Zhai Z, Shu HB. SIKE is an IKK ϵ /TBK1-associated suppressor of TLR3- and virus-triggered IRF-3

- activation pathways. *EMBO J* 2005;**24**:4018–4028.
60. Jounai N, et al. The Atg5-Atg12 conjugate associates with innate antiviral immune responses. *Proc Natl Acad Sci USA* 2007;**104**:14050–14055.
 61. Ishikawa H, Barber GN. STING is an endoplasmic reticulum adaptor that facilitates innate immune signalling. *Nature* 2008;**455**:674–678.
 62. Zhong B, et al. The adaptor protein MITA links virus-sensing receptors to IRF3 transcription factor activation. *Immunity* 2008;**29**:538–550.
 63. Gack MU, et al. TRIM25 RING-finger E3 ubiquitin ligase is essential for RIG-I-mediated antiviral activity. *Nature* 2007;**446**:916–920.
 64. Friedman CS, et al. The tumour suppressor CYLD is a negative regulator of RIG-I-mediated antiviral response. *EMBO Rep* 2008;**9**:930–936.
 65. Oshiumi H, Matsumoto M, Hatakeyama S, Seya T, Riplet/RNF135, a RING finger protein, ubiquitinates RIG-I to promote interferon- β induction during the early phase of viral infection. *J Biol Chem* 2009;**284**:807–817.
 66. Arimoto KI, Takahashi H, Hishiki T, Konishi H, Fujita T, Shimotohno K. Negative regulation of the RIG-I signaling by the ubiquitin ligase RNF125. *Proc Natl Acad Sci USA* 2007;**104**:7500–7505.
 67. Gao D, et al. REUL is a novel E3 ubiquitin ligase and stimulator of retinoic-acid-inducible gene-I. *PLoS ONE* 2009;**4**:e5760.
 68. Arimoto KI, Konishi H, Shimotohno K. UbcH8 regulates ubiquitin and ISG15 conjugation to RIG-I. *Mol Immunol* 2008;**45**:1078–1084.
 69. Tang ED, Wang CY. MAVS self-association mediates antiviral innate immune signaling. *J Virol* 2009;**83**:3420–8.
 70. Onoguchi K, et al. Virus-infection or 5'ppp-RNA activates antiviral signal through redistribution of IPS-1 mediated by MFN1. *PLoS Pathog* 2010;**6**:e1001012.
 71. Yasukawa K, et al. Mitofusin 2 inhibits mitochondrial antiviral signaling. *Sci Signal* 2009;**2**:ra47.
 72. Bowie AG, Unterholzner L. Viral evasion and subversion of pattern-recognition receptor signalling. *Nat Rev Immunol* 2008;**8**:911–922.
 73. Komuro A, Bammig D, Horvath CM. Negative regulation of cytoplasmic RNA-mediated antiviral signaling. *Cytokine* 2008;**43**:350–358.

Hepatitis C Virus Hijacks P-Body and Stress Granule Components around Lipid Droplets[▽]

Yasuo Ariumi,^{1,2*} Misao Kuroki,¹ Yukihiro Kushima,³ Kanae Osugi,⁴ Makoto Hijikata,³
Masatoshi Maki,⁴ Masanori Ikeda,¹ and Nobuyuki Kato¹

Department of Tumor Virology, Okayama University Graduate School of Medicine, Dentistry, and Pharmaceutical Sciences, Okayama 700-8558, Japan¹; Center for AIDS Research, Kumamoto University, Kumamoto 860-0811, Japan²; Department of Viral Oncology, Institute for Virus Research, Kyoto University, Kyoto 606-8507, Japan³; and Department of Applied Molecular Biosciences, Graduate School of Bioagricultural Sciences, Nagoya University, Nagoya 464-8601, Japan⁴

Received 19 November 2010/Accepted 21 April 2011

The microRNA miR-122 and DDX6/Rck/p54, a microRNA effector, have been implicated in hepatitis C virus (HCV) replication. In this study, we demonstrated for the first time that HCV-JFH1 infection disrupted processing (P)-body formation of the microRNA effectors DDX6, Lsm1, Xrn1, PATL1, and Ago2, but not the decapping enzyme DCP2, and dynamically redistributed these microRNA effectors to the HCV production factory around lipid droplets in HuH-7-derived RSc cells. Notably, HCV-JFH1 infection also redistributed the stress granule components GTPase-activating protein (SH3 domain)-binding protein 1 (G3BP1), ataxin-2 (ATX2), and poly(A)-binding protein 1 (PABP1) to the HCV production factory. In this regard, we found that the P-body formation of DDX6 began to be disrupted at 36 h postinfection. Consistently, G3BP1 transiently formed stress granules at 36 h postinfection. We then observed the ringlike formation of DDX6 or G3BP1 and colocalization with HCV core after 48 h postinfection, suggesting that the disruption of P-body formation and the hijacking of P-body and stress granule components occur at a late step of HCV infection. Furthermore, HCV infection could suppress stress granule formation in response to heat shock or treatment with arsenite. Importantly, we demonstrate that the accumulation of HCV RNA was significantly suppressed in DDX6, Lsm1, ATX2, and PABP1 knockdown cells after the inoculation of HCV-JFH1, suggesting that the P-body and the stress granule components are required for the HCV life cycle. Altogether, HCV seems to hijack the P-body and the stress granule components for HCV replication.

Hepatitis C virus (HCV) is the causative agent of chronic hepatitis, which progresses to liver cirrhosis and hepatocellular carcinoma. HCV is an enveloped virus with a positive single-stranded 9.6-kb RNA genome, which encodes a large polyprotein precursor of approximately 3,000 amino acid (aa) residues. This polyprotein is cleaved by a combination of the host and viral proteases into at least 10 proteins in the following order: core, envelope 1 (E1), E2, p7, nonstructural 2 (NS2), NS3, NS4A, NS4B, NS5A, and NS5B (12, 13, 21). The HCV core protein, a nucleocapsid, is targeted to lipid droplets (LDs), and the dimerization of the core protein by a disulfide bond is essential for the production of infectious virus (24). Recently, LDs have been found to be involved in an important cytoplasmic organelle for HCV production (26). Budding is an essential step in the life cycle of enveloped viruses. The endosomal sorting complex required for transport (ESCRT) system has been involved in such enveloped virus budding machineries, including that of HCV (5).

DEAD-box RNA helicases with ATP-dependent RNA-unwinding activities have been implicated in various RNA metabolic processes, including transcription, translation, RNA splicing, RNA transport, and RNA degradation (32). Previously, DDX3 was identified as an HCV core-interacting pro-

tein by yeast two-hybrid screening (25, 29, 43). Indeed, DDX3 is required for HCV RNA replication (3, 31). DDX6 (Rck/p54) is also required for HCV replication (16, 33). DDX6 interacts with an initiation factor, eukaryotic initiation factor 4E (eIF-4E), to repress the translational activity of mRNP (38). Furthermore, DDX6 regulates the activity of the decapping enzymes DCP1 and DCP2 and interacts directly with Argonaute-1 (Ago1) and Ago2 in the microRNA (miRNA)-induced silencing complex (miRISC) and is involved in RNA silencing. DDX6 localizes predominantly in the discrete cytoplasmic foci termed the processing (P) body. Thus, the P body seems to be an aggregate of translationally repressed mRNPs associated with the translation repression and mRNA decay machinery.

In addition to the P body, eukaryotic cells contain another type of RNA granule termed the stress granule (SG) (1, 6, 22, 30). SGs are aggregates of untranslating mRNAs in conjunction with a subset of translation initiation factors (eIF4E, eIF3, eIF4A, eIFG, and poly(A)-binding protein [PABP]), the 40S ribosomal subunits, and several RNA-binding proteins, including PABP, T cell intracellular antigen 1 (TIA-1), TIA-1-related protein (TIAR), and GTPase-activating protein (SH3 domain)-binding protein 1 (G3BP1). SGs regulate mRNA translation and decay as well as proteins involved in various aspects of mRNA metabolisms. SGs are cytoplasmic phase-dense structures that occur in eukaryotic cells exposed to various environmental stress, including heat, arsenite, viral infection, oxidative conditions, UV irradiation, and hypoxia. Impor-

* Corresponding author. Mailing address: Center for AIDS Research, Kumamoto University, 2-2-1 Honjo, Kumamoto 860-0811, Japan. Phone and fax: 81 96 373 6834. E-mail: ariumi@kumamoto-u.ac.jp.

[▽] Published ahead of print on 4 May 2011.